INTERNATIONAL JOURNAL OF HYDROGEN ENERGY 38 (2013) 14576–14594

Available online at www.sciencedirect.com

SciVerse ScienceDirect

journal homepage: www.elsevier.com/locate/he

Review

Review of electrochemical ammonia production technologies and materials

S. Giddey*, S.P.S. Badwal, A. Kulkarni

CSIRO Energy Technology, Private Bag 33, Clayton South 3169, Vic., Australia

ARTICLE INFO

Article history:
Received 20 June 2013
Received in revised form
5 September 2013
Accepted 12 September 2013
Available online 5 October 2013

Keywords:
Ammonia
Electrochemical ammonia synthesis
Haber–Bosch process
Energy storage
Hydrogen
Fuel cells

ABSTRACT

Ammonia, being a good source of hydrogen, has the potential to play a significant role in a future hydrogen economy. The hydrogen content in liquid ammonia is 17.6 wt% compared with 12.5 wt% in methanol. Although a large percentage of ammonia, produced globally, is currently used in fertiliser production, it has been used as a fuel for transport vehicles and for space heating. Ammonia is an excellent energy storage media with infrastructure for its transportation and distribution already in place in many countries. Ammonia is produced at present through the well known Haber–Bosch process which is known to be very energy and capital intensive. In search for more efficient and economical process and in view of the potential ammonia production growth forecast, a number of new processes are under development. Amongst these, the electrochemical routes have the potential to substantially reduce the energy input (by more than 20%), simplify the reactor design and reduce the complexity and cost of balance of plant when compared to the conventional ammonia production route. Several electrochemical routes based on liquid, molten salt, solid or composite electrolytes consisting of a molten salt and a solid phase are currently under investigation. In this paper these electrochemical methods of ammonia synthesis have been reviewed with a discussion on materials of construction, operating temperature and pressure regimes, major technical challenges and materials issues.

1. Introduction

Ammonia (NH_3) is an alkaline, colourless and lighter than air gas with pungent and penetrating odour. The boiling point for liquefied anhydrous ammonia is −33.3 °C at atmospheric pressure [1]. It is the second most commonly produced chemical in the world. Ammonia stays in liquid form above about 9–10 bar pressure at ambient temperature [1,2], thus it can be stored in low pressure vessels similar to those used for LPG. The conventional route of producing ammonia is by the Haber–Bosch process named after two Scientists Fritz Haber and Carl Bosch (both winning Noble prize for their contribution to the discovery and industrial process development respectively) [1,4–6]. The process requires reaction of hydrogen and nitrogen over an iron based catalyst at temperatures in the vicinity of 500 °C and pressures up to 300 bar. Over 200 million metric tons of ammonia per annum is produced by this process worldwide [7,8]. About 80% of the ammonia produced globally is used for nitrogen based fertiliser production [8]. The remaining 20% of the ammonia

* Corresponding author.
E-mail address: sarb.giddey@csiro.au (S. Giddey).
0360-3199/$ – see front matter
http://dx.doi.org/10.1016/j.ijhydene.2013.09.054

production is used in explosives, pharmaceuticals, refrigeration, cleaning products and many other industrial processes [1,8–10]. For ammonia synthesis, the source of hydrogen is mostly natural gas (NG) and involves desulphurisation, methane steam reforming followed by water gas shift reaction to convert CO to hydrogen and CO_2. The residual CO is removed by methanation reaction and CO_2 is removed by pressure swing adsorption process [1,11]. Nitrogen is typically sourced from atmospheric air by using cryogenic air separation units.

Ammonia synthesis reaction in the Haber–Bosch process is given as:

$$3H_2 + N_2 \rightarrow 2NH_3 \quad \Delta H_{300} = -46.35\,KJ/mol,\ \Delta S_{300} = -99.35\,J/K\,mol \tag{1}$$

The negative entropy of the reaction dictates that the reaction is favoured at lower temperatures, however, the high dissociation energy of triply bonded nitrogen molecule (911 KJ mol^{-1}) presents a significant activation barrier [1]. While from thermodynamic standpoint, the reaction is favoured by high pressures and low temperatures, the kinetics demands high operating temperatures to achieve reasonable ammonia production rates. The kinetic rate of Reaction (1) increases with increasing temperature, reaching maxima at a certain temperature and then decreasing if the temperature is increased further due to lower equilibrium ammonia concentration stemming from its decomposition. The temperature at which the reaction rate is maximum, obviously varies with the process pressure. For example, at a pressure of 100 bar (1 bar = 0.1 MPa), for a stoichiometric H_2/N_2 mixture, the reaction rate reaches a maximum of 0.01 kmol h^{-1} kg^{-1} at about 432 °C while increasing the pressure to 300 bar pushes the maxima to 537 °C with a reaction rate of 0.18 kmol h^{-1} kg^{-1} [1,2]. Clearly there is a need for balance between the operating temperature, pressure and the ammonia yield. Also to facilitate the activation under practically feasible pressures, the use of catalysts such as iron oxides is virtually mandatory for industrial production. Typically in industrial processes, the reaction is carried out at temperatures between 300 and 550 °C and pressures between 100 and 300 bar in the presence of reduced Fe_3O_4 based catalyst bed for reaction to proceed at reasonable rates. Since conversion rates are very low for a single pass (only 10–15% conversion of reactants), the overall plant has several catalytic beds with gases cooled after each bed, ammonia separated and unreacted gases fed to the next bed to increase overall yield. Alternatively the unreacted gases can be recycled over the same bed. The total energy consumption by this route is around 9500 kWh/ton of ammonia and increases to 12,000 kWh/ton if H_2 is produced via electrolysis of water rather than by the steam reforming of methane [9].

Ammonia is also being considered an energy storage media and a source of hydrogen as the hydrogen content in liquid ammonia is 17.6 wt% compared with 12.5 wt% in methanol [3,12–14]. Ammonia has been used as a fuel for transport vehicles as it can be combusted in an internal combustion engine, and also for space heating [3,9]. Ammonia, being a good source of hydrogen, has the potential to play a significant role in a future hydrogen economy [3,12–15]. Ammonia can be easily cracked to produce hydrogen for use in fuel cells or other hydrogen applications at end user sites. The by-products of direct ammonia combustion are water and nitrogen. Table 1 compares total volumetric and gravimetric energy content of various liquid fuels with ammonia. However, the main advantage of using ammonia as a source of hydrogen is that the volumetric hydrogen energy density in liquid anhydrous ammonia is significantly higher than that of liquid hydrogen [3,9,12,14,15]. In fact, the volumetric hydrogen energy density of ammonia is the highest amongst many common liquid fuels (methanol, ethanol, gasoline, LPG, etc.) after reforming to produce hydrogen. Ammonia can be used directly as a fuel in alkaline or high temperature fuel cells [16–19] which have good tolerance for residual ammonia levels. However, low temperature fuel cells based on acidic membranes such as Nafion are incompatible and degrade easily by ammonia concentration as low as 0.1 ppm [14].

Table 1 – Energy content of various fuels.[b]

Chemical	Energy content (HHV)[a]		Energy content (LHV)[a]	
	MJ/kg	MJ/L	MJ/kg	MJ/L
Liquid H_2	141.9	10.1	119.9	8.5
Liq NH_3	22.5	15.3	18.6	12.7
CH_3OH	22.9	18.2	20.1	15.8
C_2H_5OH	29.9	23.6	26.9	21.2
CH_4 (LNG)	56.2	23.6	50.0	20.9
LPG	47.2	25.5	43.5	23.5
Gasoline	46.5	34.6	43.1	32.1
Diesel	45.7	38.3	42.8	35.8

[a] HHV: High Heating Value, LHV: Low Heating Value.
[b] http://www1.eere.energy.gov/hydrogenandfuelcells/tech_validation/pdfs/fcm01r0.pdf, http://www.afdc.energy.gov/fuels/fuel_comparison_chart.pdf, http://www.engineeringtoolbox.com/combustion-values-d_411.html, http://www.dtic.mil/dtic/tr/fulltext/u2/638360.pdf.

Liquid ammonia storage, transportation and distribution is relatively easy due to the low pressure (~9–10 bar) at which it stays in the liquid form at room temperature and its high gravimetric density of 0.68 g ml^{-1} (at boiling point and 1 bar) compared to 0.071 g ml^{-1} for liquid hydrogen at −253 °C. From safety point of view, ammonia gas is lighter than air (just under 60% of the density of air) and if a leak does occur, ammonia dissipates into upper atmosphere quickly. Furthermore, ammonia has a strong pungent smell and can be detected by most humans in very low concentrations (20–50 ppm) [14], well below its harmful limits. The Immediately "Dangerous to Life or Health" (IDLH) concentration level is 300 ppm. Procedures for safe handling of large quantities of ammonia are well established and documented and the infrastructure for its transportation by rail, road or pipelines exists in many countries.

Due to the large number of applications and products where ammonia is utilised and increasing interest in using it as an energy storage media, a rapid growth in ammonia production capacity is expected globally. This is encouraging the development of alternative routes for ammonia production which are less energy intensive and economically more viable. Ammonia can be synthesised with a number of electrochemical routes and many different electrolytic systems are currently under development. A short review of solid state

electrochemical ammonia production methods has been published recently [20]. It has been forecast that electrochemical routes can save more than 20% of the energy consumption as compared to the conventional Haber–Bosch route [9], although none has achieved the level of technological maturity required for commercial production of ammonia. Fig. 1 compares flow diagrams of the Haber–Bosch process with an envisaged electrochemical route for ammonia production. This review will discuss recent progress made in various electrochemical processes under consideration with emphasis on materials of construction, operating temperature and pressure regimes, ammonia production and N_2/H_2 conversion rates, Faradaic efficiency and technical status of the technology.

2. Electrochemical production of ammonia

There are four main categories of electrolytes used for ammonia production as shown schematically in Fig. 2. These are based on (i) liquid electrolytes operating near room temperature; (ii) molten salt electrolytes operating at intermediate temperatures (300–500 °C); (iii) composite electrolytes consisting of a traditional solid electrolyte mixed with a low melting salt (300–700 °C); and (iv) solid electrolytes with a wide operating temperature range from near room temperature up to 700–800 °C depending on the type of electrolyte membrane used. In each type of system there is a choice for different electrode and electrolyte systems and operating conditions. In general, electrolytic cells based on solid electrolyte membrane are more versatile as these allow easy separation of hydrogen feed from ammonia product. A large number of electrochemical routes for the production of ammonia typically involve supply of hydrogen to one electrode of the electrolytic cell, formation of H^+ at the electrode/electrolyte interface, migration of protons through the electrolyte and reaction with N_2 at the other electrode to form ammonia with uptake of electrons (Fig. 3).

Hydrogen, for the electrolytic routes, like the Haber–Bosch process, can be sourced from natural gas [1] or electrolysis of water, or even decomposition of an organic liquid such as ethanol. Hydrogen from water electrolysis utilising a renewable energy source such as wind or solar would substantially reduce the carbon footprint for ammonia production [21]. In fact water can also act as a source of hydrogen inside the electrolytic cell through its reaction in the electrochemical process. The use of water as a source of hydrogen would also be helpful in eliminating any issues of catalyst poisoning due to traces of sulphur compounds or CO which are common impurities in hydrogen produced via steam reforming of natural gas. The process can be carried out under ambient conditions or at higher temperatures depending on the type of the electrolyte material used.

There are overreaching requirements on materials of use at the electrolytic cell operating temperatures and become more stringent with increasing temperature and pressure. The electrolyte must have reasonable ionic conductivity and be stable in cell operating environments. In high temperature solid state systems, matching of thermal expansion coefficient with other cell components and mechanical

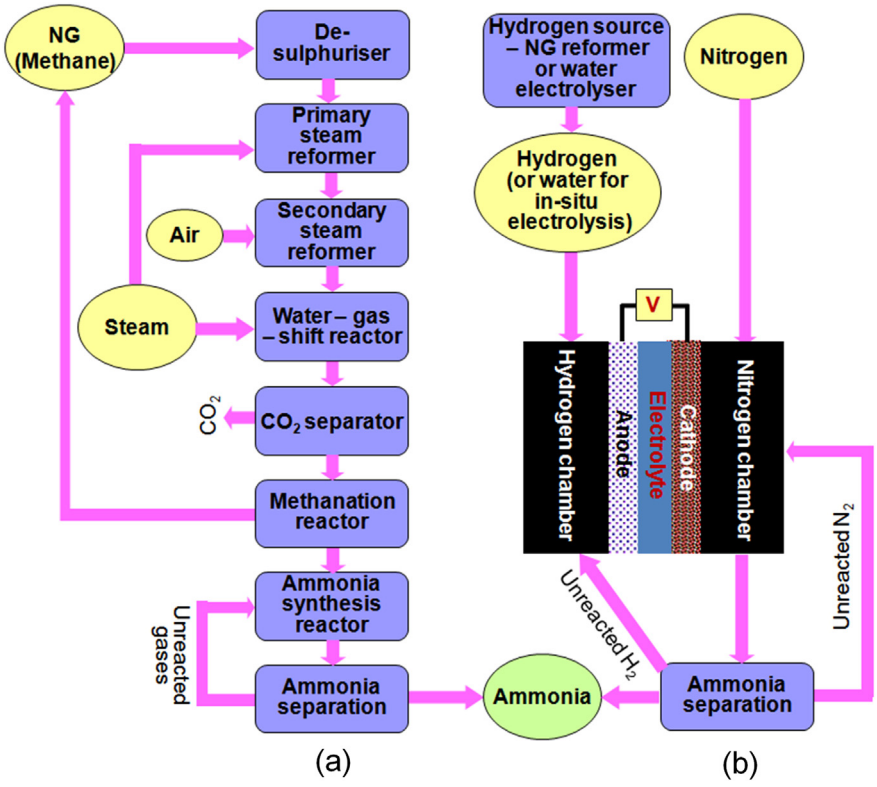

Fig. 1 – Flow diagrams comparing (a) standard Haber–Bosch process with (b) the electrochemical route for ammonia synthesis.

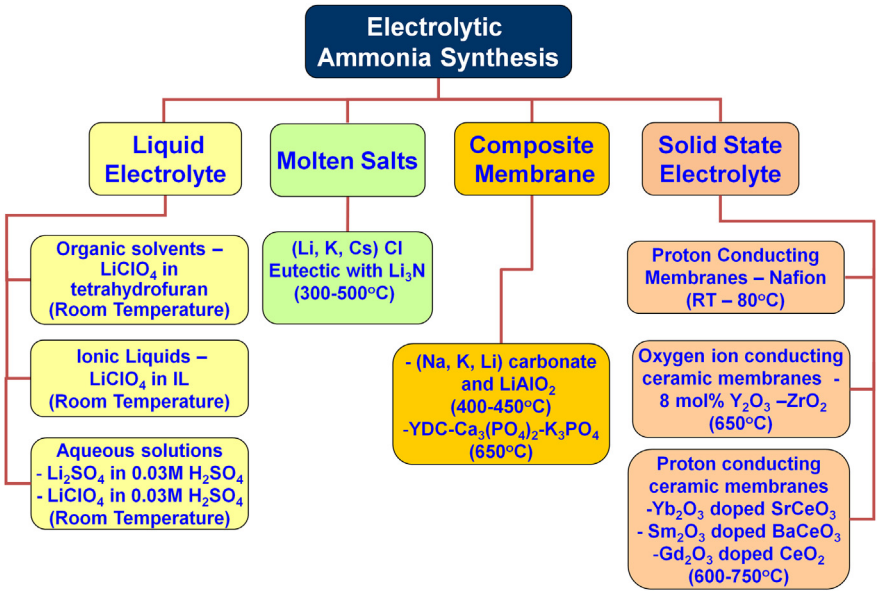

Fig. 2 – Various electrolytic options under consideration for ammonia synthesis.

properties also become critical. The cleavage of the nitrogen molecule requires breaking of three bonds and substantial energy. Thus there are stringent requirements for the nitrogen side catalyst. In terms of overall process efficiency, there is a balance between current efficiency (the % of electric current that goes towards ammonia synthesis from the total current that flowed) and ammonia production rates. For example, high current efficiency can be achieved for very low current densities, however, the ammonia production rates would be low, affecting the overall economic viability of the process.

Most electrolytic, especially solid state, processes are thermally activated with conductivity increasing and electrode reaction kinetics becoming faster with increasing temperature. However, as mentioned earlier, the ammonia production from hydrogen and nitrogen is exothermic in nature and is facilitated by high pressures and low temperatures. Thus a balance between the operating temperature, pressure and the ammonia yield needs to be established for each electrochemical system in determining ammonia production rates. For high temperature electrolytic routes for ammonia production, the use of waste heat from thermal or nuclear power plants or heat from solar/renewable energy sources would make the overall process more environmentally friendly.

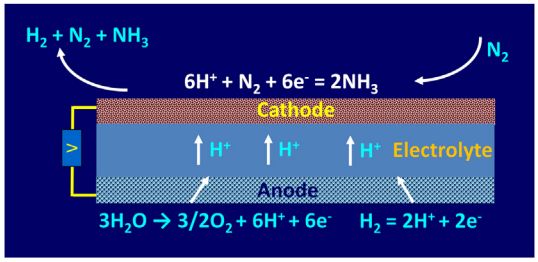

Fig. 3 – A schematic of the operating principle of electrochemical route for ammonia synthesis based on proton conducting solid electrolyte.

3. Liquid electrolyte based systems

There is very little information available in the literature on the synthesis of ammonia based on liquid electrolytes in comparison with that on solid electrolytes. Tsuneto et al. investigated the use of organic solvent based electrolytes to synthesise ammonia at near room temperatures and atmospheric pressures [22]. In their study, lithium perchlorate ($LiClO_4$ (0.2 M)) in tetrahydrofuran was used as the electrolyte with ethanol (0.18 M) as the hydrogen source. The electrolysis experiments were performed at 2 mA cm^{-2} at room temperature and atmospheric pressure with different metal cathodes (Ti, Mo, Fe, Co, Ni, Cu, Ag). Hydrogen was produced in addition to ammonia with an overall current efficiency of 5–8% for ammonia production. The current efficiency was very much dependent on the type of metal used as the cathode and the source of hydrogen (ethanol, methanol, water, acetic acid, 1-propanol, 2-propanol, etc.) and its concentration for ammonia synthesis. For ethanol, the maximum efficiency was achieved at 0.18 M concentration. The current efficiency for ammonia production improved significantly but decreased for the competing reaction of hydrogen production with increasing nitrogen pressure. A current efficiency of ~58% for ammonia production was achieved when iron was used as a cathode at an operating temperature of 50 °C and when nitrogen was supplied to the cathode at a pressure of 50 atm. These observations indicate that around 58% of the current supplied through the electrolyte was converted to a useful product. i.e. ammonia. The ammonia production rate for these operating conditions was calculated to be around 4.0×10^{-9} mol cm^{-2} s^{-1}.

The presence of water was indicated to inhibit the production of NH_3 and therefore should be excluded if high ammonia synthesis rates are to be achieved. Thus Pappenfus et al. used hydrophobic ionic liquids as electrolyte solvents with $LiClO_4$ as the source of Li^+ ions for ammonia synthesis [23]. Ethanol was used as the proton source and synthesis reaction was performed on Ni plate cathode (area of 2 cm^2) with same size Pt plate being used as the anode. The experiments were performed at an ambient temperature and atmospheric pressure. A very low current efficiency of 3–5% was achieved considering that the current density was also low (2 mA cm^{-2}). The current efficiency may improve under a different set of experimental conditions (e.g. high pressures), however, under the conditions of test, breakdown of the ionic liquid electrolyte was observed indicating serious concerns about the long term viability of the process. Furthermore the solubility of Li salts has been reported to be low in many ionic liquids [23].

Besides $LiClO_4$, Tsuneto et al. evaluated a number of other salts such as $LiBF_4$, $Li(CF_3SO_3)$, $NaClO_4$ and Bu_4NClO_4. A maximum current efficiency of 59.8% was achieved with $Li(CF_3SO_3)$ in tetrahydrofuran and ethanol at a nitrogen pressure of 50 atm [22]. A negligible amount of ammonia was detected when $NaClO_4$ and Bu_4NClO_4 salts were used confirming the Li mediated reaction mechanism. In all cases discussed above, the mechanism proposed is somewhat unclear and has been suggested as follows. The Li^+ deposits as metallic Li at the cathode which reacts with nitrogen to form Li_3N. This material then reacts with ethanol to form NH_3 as per reaction: $3C_2H_5OH + Li_3N = NH_3 + 3LiOC_2H_5$. The side reaction may be a direct reduction of the protic material such as ethanol ($2EtOH + 2e^- = H_2 + 2EtO^-$) or through reaction with Li deposited on the cathode ($2Li + 2EtOH = 2EtOLi + H_2$). For highly protic hydrogen sources such as acetic acid and methanol, the side reactions appeared to dominate the overall process [23]. Although the overall principle of the process has been clearly established, the technology is at very early stage of development with only small size cells evaluated in the laboratory and for a limited period of time. Furthermore, there was no discussion on the reaction mechanism at the anode, and from a technology perspective, how the system would function as a complete cell. There was no data on electrode polarisation losses or operation over a period of time.

Ammonia production has also been investigated in aqueous system (0.1 M Li_2SO_4/0.03 M H^+ solution) at 60 bar nitrogen pressure using polypyrrole electrode [24] or in methanol + $LiClO_4$ electrolyte with 0.03 M H_2SO_4 with polyaniline coated Pt electrode at 50 bar nitrogen pressure [25]. The maximum ammonia yield was reported to be 53 μmol in 5 h for an 8 cm^2 active area cell (calculated to be 3.68×10^{-10} mol cm^{-2} s^{-1}) at 60 bar nitrogen pressure [24].

4. Molten salt based electrolyte systems

Electrolysis cells based on a molten salt as the electrolyte for ammonia generation have been reported with operating temperature between 300 and 500 °C. Murakami et al. used an eutectic of LiCl, KCl and CsCl as the electrolyte with Li_3N (0.5 mol%) dissolved in the electrolyte as the source for nitride ions (N^{3-}) [26]. With porous Ni as the working and counter electrodes, nitrogen supplied to the cathode was reduced to N^{3-} and hydrogen supplied to the anode reacted with nitride ions to form ammonia ($N^{3-} + 1.5H_2 = NH_3 + 3e^-$) as shown in Fig. 4. The side reaction was the evolution of nitrogen through direct oxidation of nitride ions. These authors obtained an ammonia production rate of 3.3×10^{-9} mol cm^{-2} s^{-1} at 400 °C with a current efficiency of 72%. In a modification to the above reaction Murakami et al. used methane as the source of hydrogen and studied its direct reaction with nitride ions in the LiCl, KCl and CsCl eutectic with dissolved Li_3N as the electrolyte [27]. Nitride ions reacted with CH_4 as per reaction ($N^{3-} + 3/4CH_4 = NH_3 + 3/4C + 3e^-$). The formation of both carbon and ammonia was confirmed at 500 °C, however, the rate of this reaction was negligible at 400 °C. The competing reaction of nitrogen evolution at the anode was observed at both temperatures although it was the dominant reaction at 400 °C.

Murakami et al. in a separate study investigated the use of water vapours as a source for hydrogen employing LiCl–KCl–CsCl eutectic as the electrolyte to synthesise ammonia [28,29]. The molten salt contained 0.5 mol% lithium nitride and the synthesis was performed at 300 °C. Porous nickel was used as the cathode and either glassy carbon or boron doped diamond as the anode of the cell. Water and nitrogen were used as reactants. Nitrogen was supplied to the cathode and after getting reduced to nitride ions, reacted with water to produce ammonia, and oxide ions as follows: $3/2H_2O + N^{3-} \rightarrow NH_3 + 3/2O^{2-}$. The oxide ions formed above reacted with glassy carbon to form CO_2 [28], whereas boron doped diamond was essentially a non-consumable anode and O^{2-} ions were removed from the melt in the form of oxygen at the anode as per the following reaction: $3/2O^{2-} \rightarrow 3/4O_2 + 3e^-$ [29]. The process is schematically shown in Fig. 5. The current efficiency for the ammonia synthesis reaction (the % of electric current that went towards ammonia synthesis from total current that flowed) was around 23% with glassy carbon [28]. It was significantly lower (~10% after 30 min of electrolysis) for boron doped diamond anode [29] with the balance of the current contributing to nitrogen formation through the oxidation of nitride ions ($N^{3-} \rightarrow 1/2N_2 + 3e^-$). No information on ammonia production rates was given.

In a variation to the above approach, Murphy et al. have proposed that the process can be further improved if both nitrogen and hydrogen gases are supplied at the cathode, and are then reduced to nitride and hydride ions respectively [30].

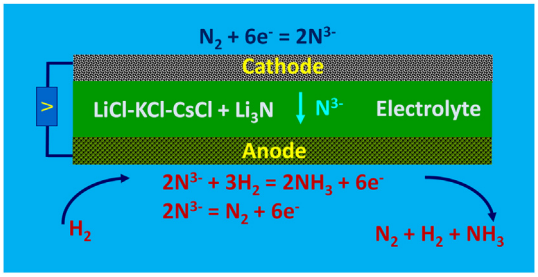

Fig. 4 – A schematic of the operating principle of electrochemical route for ammonia synthesis based on molten salt electrolyte.

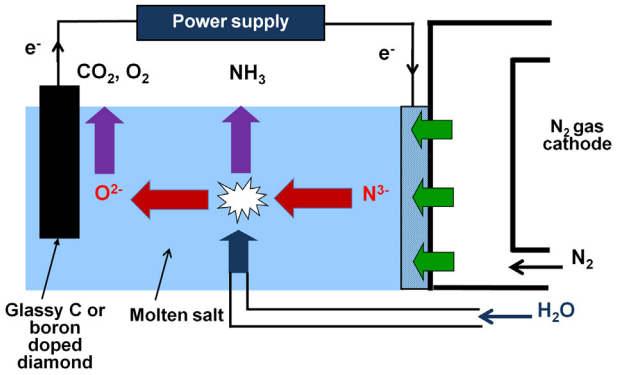

Fig. 5 – A schematic of the electrochemical route for ammonia synthesis based on molten salt electrolyte with water as the source for hydrogen [27,28].

These ions present in the electrolyte are then oxidised and adsorbed at the anode as nitrogen and hydrogen atoms, and then react to produce ammonia. It was proposed that practical systems based on this principle can consist of lithium nitride and lithium hydride in a porous matrix such as $LiAlO_2$ as the electrolyte, and porous graphite, metal or alloy as the cathode and anode. It has been suggested that this type of cell arrangement may not suffer from low H^+ fluxes and low conversions as observed with other such proton conducting electrolytic cells.

A number of concepts, where hydrogen, methane or water was used as the reactant, have been demonstrated on small cells in laboratory experiments of short duration (minutes). The technology is at an early stage of development with a good current efficiency of 72% reported for hydrogen oxidation reaction and ammonia synthesis rates of about 3.3×10^{-9} mol cm^{-2} s^{-1} [26].

5. Composite membrane based systems

The composite electrolytes consist of one or more different ionic conducting phases and the second or third phase is added to the parent phase to modify electrical, thermal or mechanical properties. For example, an alkali metal carbonate and an oxide such as $LiAlO_2$ or Sm_2O_3 doped CeO_2 have been shown to have oxygen-ion, carbonate ion and even proton conductivity under certain conditions (e.g. in the presence of hydrogen) [31,32]. Similarly yttrium doped ceria (YDC)–$Ca_3(PO_4)_2$–K_3PO_4 composite electrolyte has been shown to have proton conductivity [33]. In these cases, the ionic conductivity is improved by the addition of a low melting salt phase to the oxide. Such materials have been under investigation as potential electrolytes for intermediate temperature (400–800 °C) fuel cells and are also being employed to study ammonia production rates under a range of operating conditions.

Amar et al. used a mixture of Na, K and Li carbonates in 50:50 weight ratio, with $LiAlO_2$ composite as an electrolyte to investigate performance of a spinel ferrite $CoFe_2O_4$ as the ammonia synthesis catalyst [32]. It was proposed that the proton conduction in the electrolyte is via exchange of protons between CO_3^{2-} and HCO_3^- ionic species. The spinel ferrite, mixed with silver paste to enhance conductivity and to increase adhesion to the electrolyte, was used as the cathode (ammonia synthesis side) and Ag–Pd paste (20 wt% Pd) was used as the anode catalyst for hydrogen dissociation. Wet high purity hydrogen was fed to the anode and oxygen free nitrogen to the cathode. These authors achieved a peak ammonia production rate of 2.32×10^{-10} mol cm^{-2} s^{-1} at 400 °C, at an optimal cell operating voltage of ~0.8 V. However, the ammonia production rate decreased with increasing temperature being close to 9.4×10^{-11} mol cm^{-2} s^{-1} at 450 °C possibly due to ammonia decomposition. The low ammonia synthesis rates were attributed to the very small catalyst/electrolyte active area of 0.45 cm^2 and low catalytic activity of the $CoFe_2O_4$–Ag electrode material.

Amar et al. have also reported a maximum ammonia production rate of 5.39×10^{-9} mol cm^{-2} s^{-1} at 450 °C and 0.8 V using $La_{0.6}Sr_{0.4}Fe_{0.8}Cu_{0.2}O_{3-\delta}$–$Ce_{0.8}$–$Sm_{0.2}O_{2-\delta}$ on the cathode side as the ammonia synthesis catalyst [34]. $Ce_{0.8}Sm_{0.2}O_{2-\delta}$ mixed with Li, Na and K carbonate mixture in the 70:30 weight ratio was used as the electrolyte and Ni–$Ce_{0.8}Sm_{0.2}O_{2-\delta}$ as the anode in small size cells [34]. The experimental set-up and operating conditions were similar to those described above [32]. In this study Amar et al. report initially an increase in the ammonia synthesis rate from 400 to 450 °C as the proton conductivity of the composite electrolyte increased and then a decrease above this temperature due to ammonia decomposition.

Wang et al. have studied the yttrium doped ceria (YDC)–$Ca_3(PO_4)_2$–K_3PO_4 composite electrolyte (80 wt% YDC and 20 wt% binary phosphates) as a proton conducting electrolyte for ammonia production [33]. Although no information on the mechanism of oxygen-ion or protons conduction was given, the total conductivity of the composite was significantly higher as compared to the parent YDC material. Instead of using hydrogen as the reactant gas, natural gas was used as the source of hydrogen with nitrogen supplied to the cathode. Pd–Ag was used as both the anode and the cathode. The peak ammonia production rate achieved was 6.95×10^{-9} mol cm^{-2} s^{-1} at 650 °C, at an optimal cell operating voltage of ~1 V. According to these authors, methane at the anode, is converted to C_2H_6 and C_2H_4 with the release of hydrogen, and protons, on ionisation of this hydrogen at the anode/electrolyte interface, are transported through the electrolyte and react with nitrogen at the cathode/electrolyte interface (Fig. 6). Chemical analysis of the spent gas from the anode compartment showed a small increase in the concentration of C_2H_4, C_2H_6 and C_3H_8, however, most of the methane remained unreacted.

6. Ceramic/inorganic proton conducting solid electrolyte based systems

A number of different systems, based either on proton or mixed proton/oxygen-ion conducting solid electrolytes, are undergoing research and development for application in electrochemical ammonia synthesis. The basic principle of ammonia generation with solid state proton conducting membranes is essentially the same as that shown in Fig. 3 and various systems are discussed below.

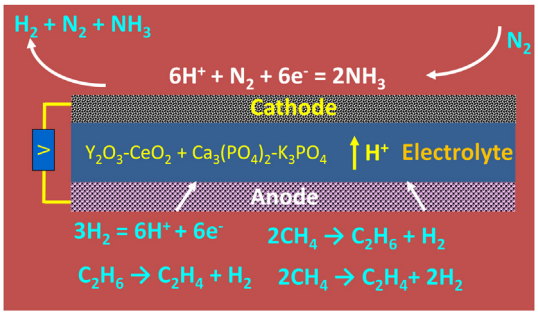

Fig. 6 – A schematic of the ammonia production method employing a composite electrolyte consisting of 80 wt% Y_2O_3–CeO_2 + 20 wt% binary phosphates as a proton conducting electrolyte and methane as the source for hydrogen.

6.1. *Ceramic proton conducting materials*

The proton conducting ceramics form an important class of electrochemical materials which have been under investigation for some time for several potential applications such as hydrogen separation membranes, intermediate temperature solid oxide fuel cells (ITSOFCs), hydrogen pumps and gas sensors [35,36]. The protonation of ceramics by dissolution of hydrogen and water vapours in the lattice to form interstitial protons was first proposed by Stotz and Wagner in 1960s based on studies on changes in the electrical resistance of Cu_2O, CoO and NiO at 900–1000 °C in hydrogen/H_2O atmospheres [37]. Subsequently there have been some literature reports on proton conductivities of oxides such as ThO_2–Sm_2O_3 solid solutions, however, most of these materials were unsuitable for practical applications due to the low proton conductivity [38]. Appreciable proton conductivity in ceramics was first demonstrated by Iwahara et al. in $SrCeO_3$ perovskites doped with aliovalent cations [39]. Since the pioneering work by Iwahara, proton conductivity has been investigated in several oxide families, however, only a limited number of oxide structures have demonstrated significant proton conductivities at operating temperatures. For applications in electrochemical devices such as fuel cells and solid electrolysers, three oxide families namely perovskites, fluorites and pyrochlores are under consideration. In addition, there is a range of other inorganic proton conducting materials which have been studied for different applications.

6.1.1. *Perovskites*

Perovskites have an ABO_3 structure with B-site atom in octahedral coordination with oxygen atoms and A-site atom at the centre as shown in Fig. 7(a). In most of the proton conducting electrolytes, A is divalent (e.g. Ba^{2+} or Sr^{2+}) and B is tetravalent cation (e.g. Zr^{4+}, Ce^{4+}) with doping at both sites with aliovalent cations. Although a perovskite is symmetrical cubic structure, in reality most of the perovskite structures are pseudocubic because of titling of the BO_6 octahedral, and displacement of cations from the ideal positions. These materials when doped with aliovalent cations demonstrate interesting defect structure with high concentration of oxygen vacancies compensated by charge carriers leading to dramatically different electrical and chemical properties. There is no significant structural change reported so far for these materials with doping, however, the temperature induced phase change from orthorhombic (300 °C) to rhombohedral (500 °C) to cubic (950 °C) structures is evident in perovskites such as cerates [40].

Trivalent ions (Nd^{3+}, Y^{3+}, Yb^{3+}, La^{3+} etc.) doped cerates such as $YBaCeO_3$ and zirconates such as $YBaZrO_3$ are perhaps some of the most studied proton conductor perovskites for various electrochemical applications. The protonic conductivities from 10^{-4} to 10^{-1} S cm^{-1} have been reported for these materials in wet H_2 atmosphere in the temperature range of 400–900 °C [41–43]. Typically ceria based perovskites demonstrate higher protonic conductivity than zirconia based oxides, however, the zirconates are chemically more stable and possess higher mechanical strength, a situation somewhat similar to zirconia and ceria based oxygen ion conductors. The basic Group II cation constituents of these materials will react with acid species such as CO_2 or SO_2 leading to the decomposition of the perovskite structure [44]. Improving the stability of these perovskites is one of the major challenges in the practical application of these materials and various approaches have been taken to improve the structural stability while maintaining the conductivity. The solid solutions of zirconia and ceria exhibit more stability compared to cerates and higher conductivity than zirconates, however, the proton conductivity still remains lower than cerates. The other approach is to use complex or mixed perovskites with general formulas $A_2(B'B'')O_6$ and $A_3(B'B_2'')O_9$. Here B″ is a pentavalent cation such as Nb [45] in both types of perovskites, and B′ is a trivalent cation (such as Sc) and divalent cation (such as Ca) respectively in $A_2(B'B'')O_6$ and $A_3(B'B_2'')O_9$ perovskite. A complex perovskite of type $A_2(B'B'')O_3$ (e.g. $Ba_2(NbEr)O_6$) has been reported to be more stable in comparison with simple perovskites and is attributed to smaller Madelung lattice energies in these perovskites [46]. The Madelung lattice energy calculation also indicates that a partial substitution of Ce in Ba cerate would enhance the stability which indeed is seen in ceria–zirconia mixed oxides. The conductivity of these oxides can be tuned using nonstoichiometric compositions by varying the B′ and B″ cations and doping levels. Further it was observed that the conductivity increases significantly with increased difference in B′ and B″ cations radii. For example in nonstoichiometric double perovskite $Sr_2(B'_{1.1}Nb_{0.9})O_{6-\delta}$ (B′ = Sc, Nd), the protonic conductivity is higher by almost four orders of magnitude when B site ion is Nd as compared to Sc [47,48]. Also the role of A-site cation is evident with Ba based complex oxides showing higher conductivities as compared to Sr based oxides, which is true for simple perovskites as well. However, to date the conductivities and conduction activation energies of these complex perovskites are found to be lower than best reported values for Ba cerates [48].

Besides the stability, a high sintering temperature (~1700 °C) required to achieve dense materials, particularly for the zirconate based proton conductors, is another major issue. The sintering characteristics can be improved with the addition of sintering aids such as ZnO, NiO, CuO in small molar concentrations [49–52]. Park et al. reported that the co-doping of Yb-doped $BaZrO_3$ with 1.0 mol% of CuO results in a dense single phase perovskite at a sintering temperature of 1500 °C as compared to 1700 °C for the specimen without CuO

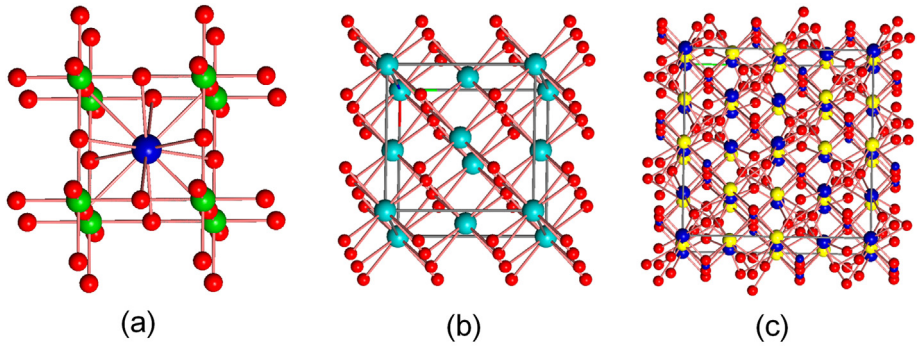

Fig. 7 – Crystal structure schematics for (a) Perovskites, (b) fluorites and (c) pyrochlores. Oxygen atoms are coloured red in all diagrams, metal atoms are coloured: (a) green – B-site, Blue – A-site; (b) turquoise – metal atoms; (c) yellow – A-site, blue – B-site. Figures produced using Xtaldraw Software© 1997 Bob Downs and Kurt Bartelmehs. Written permission obtained from the copyright owner. (For interpretation of the references to colour in this figure legend, the reader is referred to the web version of this article.)

[52]. The doping with CuO resulted in a change of phase from orthorhombic to cubic structure while maintaining the conductivity of 5.5×10^{-3} S cm^{-1} at 600 °C under the wet nitrogen atmosphere [52]. Recently Tao et al. reported that doping with a small amount of ZnO (0.04 mol%) formed high density single phase $BaZr_{0.8}Y_{0.2}O_{3-\delta}$ zirconate at 1325 °C after 10 h of sintering, while this material without ZnO did not sinter fully even at 1600 °C [53]. Furthermore, ZnO doped mixed perovskite ($BaCe_{0.5}Zr_{0.3}Y_{0.16}Zn_{0.04}O_{3-\delta}$) demonstrated considerable stability in the presence of CO_2 after cycling up to 1200 °C [53]. The total conductivity of 10 mS cm^{-1} was reported at 600 °C in 5% H_2 (amongst the highest conductivity value for single phase ceramic proton conductors at this temperature) making these material promising candidates for electrochemical applications. Similar studies have been reported with indium doped Ba zirconate (BZI) electrolytes resulting in total conductivity up to 10 mS cm^{-1} at 650 °C [54]. Fully dense single phase perovskite thick film was fabricated at 1400 °C on anode substrate and tested in a fuel cell to deliver power densities up to 85 mW cm^{-2} at 700 °C with $Sm_{0.5}Sr_{0.5}CoO_{3-\delta}$–$Ce_{0.8}Sm_{0.2}O_{2-\delta}$ (SSC–SDC) as the cathode material [54]. Most of the sintering aids improve the sinterability while maintaining the conductivity, however, doping with materials such as PrO_x may introduce a mixed conductivity regime because of the variable oxidation state of Pr [55]. Since mixed conduction in the material would be detrimental to some electrochemical applications such as fuel cells and ammonia synthesis electrochemical cells, while desired in other applications such as hydrogen separation membranes, sintering aid should be chosen carefully with overall defect chemistry considerations. While alkali metal doped cerates and zironates remain major perovskites, doubly doped lanthanum gallates like $La_{0.9}Ba_{0.1}Ga_{1-x}Mg_xO_{3-\delta}$ have also shown proton conductivities in the range 10^{-4} to 10^{-2} S cm^{-1} at temperatures in the range 400–800 °C, however, more investigations are required to firmly establish the stability of these compounds [56].

6.1.2. *Fluorites*

Many ceramic oxides have a fluorite structure with the oxygen ions in cubic packing and tetravalent metal cations in alternate cube centres (Fig. 7(b)). Materials such as doped zirconia, ceria and thoria which have the fluorite structure have been studied widely as oxygen ion conducting electrolytes for solid oxide fuel cells, sensors and other similar electrochemical systems. Some of these oxides also exhibit significant mixed protonic–electronic conductivity in hydrogen rich atmospheres. Trivalent ion doped ceria constitutes a major group of proton conducting oxides with proton conductivity up to 0.0038 S cm^{-1} at a temperature of 650 °C [57]. Other significant fluorite-type oxide is lanthanum tungsten oxide ($La_{5.8}WO_{11.7}$) [58], which exhibits proton conductivity from 1 mS cm^{-1} to 10 mS cm^{-1} in the temperature range of 600–1000 °C with proton transference number of 0.7–0.9. Fluorites are in general stable materials at intermediate temperatures and not susceptible to acidic environment of CO_2/SO_2, however, long term stability of these materials in hydrogen atmosphere at high temperatures needs to be investigated.

6.1.3. *Pyrochlores*

Pyrochlores have ordered fluorite structure (sometimes also referred as fluorite superstructures) with general formula $A_2B_2O_7$ with A and B as trivalent and tetravalent cations (Fig. 7(c)). Significant proton dissolution has been observed in pyrochlores such as Ca doped lanthanum zirconates ($(La_{1.95}Ca_{0.05})Zr_2O_{7-\delta}$) and proton conductivity up to 0.068 S cm^{-1} at 600 °C has been reported [59]. The dopant (Ca^{2+}) can be introduced at either La (A-site) or Zr (B-site) site, however, doping at A-site results in higher protonic conductivity. Although the stability of pyrochlores is good, the proton conductivity is observed at only lower temperatures (<600 °C) while at higher temperatures the oxygen ion transport number increases almost exponentially and reaches 0.9 at 900 °C. These materials have been reported to show mixed conduction due to positive holes, oxygen ions and protons in wet oxygen atmosphere in the temperature range 700–900 °C. The proton transport number observed for ($(La_{1.95}Ca_{0.05})Zr_2O_{7-\delta}$) at 700 °C was 0.17. Another issue for these materials is the high sintering temperatures, in excess of 1600 °C, required to achieve high densities.

6.1.4. *Other materials*

Besides the three families of ceramic proton conductors discussed above, proton conduction is also observed in several

other oxides such as brownmillerite ($Ba_2In_2O_5$), eulytite ($Bi_4(SiO_4)_3$), and monazite ($Ln_{0.99}Sr_{0.01}PO_4$), however, the proton conductivity of these oxides is typically an order of magnitude lower than that in perovskites and fluorites [42]. While higher proton conductivity is desired for all electrochemical applications, it is particularly important for electrolytic ammonia synthesis, to achieve high ammonia synthesis rates and negate the effect of any decomposition of ammonia back to N_2 and H_2 (see Section 2). A number of other proton conducting materials have been investigated and a detailed discussion on these materials is beyond the scope of this review and readers are referred to references [35,36,42].

The temperature dependant electrical conductivities of some prospective proton and oxygen ion conducting electrolyte materials for ammonia synthesis are shown in Fig. 8.

6.2. *Mechanism of proton conduction in ceramic oxides*

It is well known that ionic conduction in solid electrolytes is governed by the lattice defect chemistry and defect reactions. In the case of ceramic proton conductors a theory of formation of hydroxyl group and a proton by dissolution of water (steam) in oxygen vacancies of host lattice is widely accepted [35,60]. The reaction involves replacement of oxygen vacancy in the lattice by hydroxyl group as follows:

$$H_2O(g) + V_{\ddot{o}} + O_o^x \rightarrow 2OH_{\dot{o}} \quad (2)$$

and dissolution of protons into lattice with maintenance of electro-neutrality by electron formation as:

$$H_2(g) + 2O_o^x \rightarrow 2OH_{\dot{o}} + 2e' \quad (3)$$

The hydroxyl defect formation or hydration reaction in ceramics is acid base type reaction, which does not involve electronic defects. The extent of protonation by above reactions depends on the basicity of host cations and the distortion in the oxide sublattice. Once the proton is formed, its diffusion takes place via Grotthuss mechanism [61,62]. It is a two-step mechanism involving reorientation of proton associated with oxygen atom (orientation step) followed by bonding with neighbouring oxygen atom (transfer step). The mechanism is shown schematically in Fig. 9. The two step mechanism of proton conduction via proton jumps between neighbouring oxygen atoms and rotational diffusion appears to be reasonably supported by data from inelastic neutron diffraction (INS) and Quasielastic neutron scattering (QENS) experiments on various proton conductors [63]. The magnitude of the activation energies for these two steps is composition dependant. Molecular Dynamics simulations reveal that for Sr doped cerate ($SrCeO_3$), both orientation and transfer steps have similar magnitude of activation energies, while for Ba doped cerate ($BaCeO_3$) only transfer step appears to be rate limiting resulting in lower overall activation energy for proton conduction of 0.50 eV as compared to 0.63 eV in Sr-cerate [64]. The deviation from ideal cubic symmetry (as is the case with $SrCeO_3$) in perovskites leads to reduction of the concentration and mobility of protonic defects [65]. The reduction in the structure symmetry changes proton diffusion paths, and causes unfavourable jumps resulting in reduction in the proton diffusion coefficient.

The Reaction (2) dictates that overall proton conduction would be energetically favoured by increasing the number of oxygen vacancies in the host lattice. Indeed it has been observed for rare earth oxides that the enthalpy of the Reaction (2) is negative and it increases (negatively) with the increasing amount of the dopant which leads to increased concentration of vacancy defects [66]. Although it might appear that increasing dopant concentration would enhance the protonic conductivity, one should also take into consideration the trapping effect due to electrostatic attraction of positively charged protons and oxygen vacancies to more negative acceptor dopants leading to additional energy barrier for proton transport [62]. Further, the trapping of the oxygen vacancies can also affect the proton concentration due to unavailability of oxygen vacancies for the hydration Reaction (2).

The proton conduction mechanism discussed above, although developed mainly for perovskites, it may be equally applicable to other structures such as fluorites. However, the overall proton conduction mechanism is somewhat unclear in

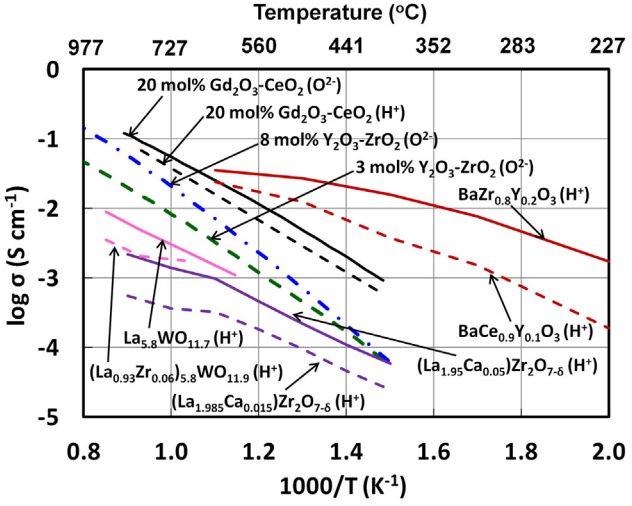

Fig. 8 – Proton and oxygen ion conductivity of various ceramic electrolytes for ammonia synthesis. 20 mol% Gd_2O_3–CeO_2 (O^{2-}), 8 mol% Y_2O_3–ZrO_2 (O^{2-}), 3 mol% Y_2O_3–ZrO_2 (O^{2-}) – authors data; 20 mol% Gd_2O_3–CeO_2 (H^+) – [57]; $BaZr_{0.8}Y_{0.2}O_3$ (H^+), $BaCe_{0.9}Y_{0.1}O_3$ (H^+) – [61]; $(La_{1.95}Ca_{0.05})Zr_2O_{7-\delta}$ (H^+), $(La_{1.985}Ca_{0.015})Zr_2O_{7-\delta}$ (H^+) – [59]; $La_{5.8}WO_{11.7}$ (H^+), $(La_{0.93}Zr_{0.06})_{5.8}WO_{11.9}$ (H^+) – [58].

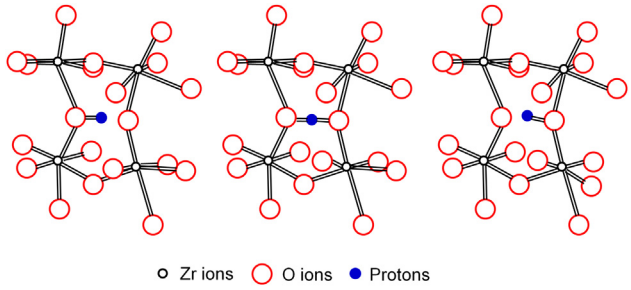

Fig. 9 – Schematic showing inter-octahedra proton hopping mechanism in orthorhombic $CaZrO_3$ structure (Figure redrawn from Ref. [61]). Ca ions are not shown for clarity. The reader is referred to the web version of the manuscript for interpretation of colours.

fluorite type oxides with smaller grain sized microstructures. While significant protonic conductivities have been observed in these materials at lower temperatures, the conduction pathways are attributed to grain boundaries instead of bulk defect diffusion [67–69]. Recently Pardes et al. studied the proton conduction behaviour in nanocrystalline doped ceria (grain size of 10–15 nm) at low temperature (200 °C) [70]. These authors demonstrated that the proton conduction is independent of the dopant concentration, while the O^{2-} conductivity was found to be directly dependant on dopant concentration confirming the existence of dominant grain boundary or interfacial proton conduction paths in nanocrystalline fluorites. Interface enhanced conduction in such systems has also been reported for other oxygen ion conductors such as nano-scale ceria zirconia composite or multilayer systems [71,72]. The proton conductivity observed at these temperatures is too low (10^{-8} to 10^{-7} S cm^{-1}) [70] for practical applications, however, above observations are important for understanding the fundamental mechanism of proton conduction and it also opens up a possibility for designing composite or heterophase electrolytes with enhanced proton conductivities.

Based on the defect chemistry and Nernst–Einstein relation, the rate of proton transport or flux can be calculated for proton conducting membranes [60]. In general the proton flux in MIEC membranes (mixed proton, oxide ion, and electron conductor) can be given by:

$$j_{H^+} = \frac{-RT}{F^2 L} \int_{downstream}^{upstream} \sigma_H \left[2(t_{O^{2-}} - t_e) d\ln p_{H_2} + t_{O^{2-}} d\ln p_{O_2} \right] \quad (4)$$

where F is Faradays constant, L is thickness of the membrane; t is transport number of particular species and σ_H is the proton conductivity; pH_2 and pO_2 are partial pressure of hydrogen and oxygen respectively. The above equation can be suitably modified to obtain hydrogen flux if electronic or O^{2-} conductivity is absent.

6.3. *Electrolytic ammonia synthesis with ceramic proton conductors*

The electrochemical ammonia generation technology, despite its enormous potential, is still in the early stage of research and development, and the investigations are mainly restricted to lab scale studies on small cells. A typical electrolytic cell for ammonia synthesis is fabricated by depositing electrode (catalyst) coatings on both sides of the proton conducting membrane. These porous electrodes are typically screen printed or brush coated on ceramic proton conductor membranes followed by heat treatment. The current collection is achieved by placing metallic meshes or sheets in contact with these electrodes. Water or hydrogen is fed to the anode and nitrogen to the cathode, and ammonia is produced on the cathode side of the cell. Clearly the proton conducting ceramic membrane, along with cathode or ammonia synthesis catalyst, are most critical components in these systems. These membranes are required to exhibit significant proton conductivity at temperatures above 400 °C. While higher operating temperatures favours the electrode reactions such as the oxidation of hydrogen into protons at the anode and subsequent proton migration through the membrane to the cathode, the ammonia synthesis reaction, being exothermic in nature, is thermodynamically less favoured. Therefore, an optimisation of the operating temperature of the cell for sufficient proton conductivity of the membrane, fast electrode kinetics and achieving NH_3 synthesis rates sufficiently higher than its dissociation (back to N_2 and H_2) remains a critical challenge for ceramic membrane reactors.

The proton conducting ceramics have been studied widely as fuel cell electrolytes and gas separation membranes, however, the literature reports on electrolytic synthesis of ammonia using these membranes are relatively scarce. In 1996, Panagos et al. modelled the process of solid state electrolytic ammonia synthesis with Yb doped Sr-cerate as the proton conducting membrane [73]. The model studies revealed that the electrochemical ammonia synthesis yields can be orders of magnitude higher than those obtained in a conventional ammonia synthesis reactor. Subsequently Marnellos et al. investigated ammonia generation by using ytterbium doped strontium cerate ($SrCe_{0.95}Yb_{0.05}O_{3-\delta}$) (SCY) closed-end tube cell with a wall thickness of 1.5 mm as the electrolyte membrane [74,75]. Pd foil was used as the electrode/current collector inside and outside the tube. Fig. 10(a) shows a schematic view of the set-up employed in this investigation. The ammonia flux rate of 3.1×10^{-9} mol cm^{-2} s^{-1} was obtained at 570 °C with current efficiency close to 75% with respect to H^+ ions transported through the membrane. The major issues encountered were the decomposition of ammonia back to hydrogen and nitrogen leading to net conversion efficiency of ~50%. The decomposition of ammonia in electrolytic cell was determined quantitatively, by feeding in the mixture of ammonia and nitrogen in helium at a rate comparable to the electrolytic synthesis. It was found that the ammonia decomposition rate decreased linearly with increasing current and reached 15% as compared to 25% at OCV with no current flow. Further, the authors reported that no NEMCA (Non-Faradaic electrochemical modification of catalytic activity) effect (at flux $\leq I/2F$) was observed in this cell arrangement (double chamber cell). The rate limiting reactant was moles of protons transported for conversion as number of moles of NH_3 produced were independent of the N_2 pressure. The

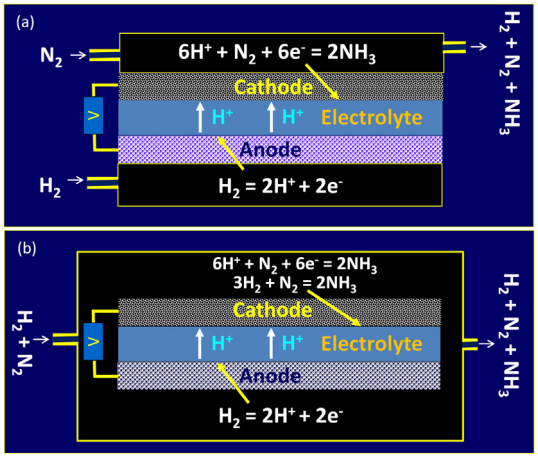

Fig. 10 – Schematic of the electrochemical cell using ceramic proton conducting electrolyte membrane (a) double chamber and (b) single chamber reactor setup.

authors also conducted investigations with a single chamber cell arrangement as shown in Fig. 10(b) [74,75]. A strontium cerate doped with ytterbium (SCY) electrolyte disc of thickness 1–2 mm was used with Pd electrodes. In this arrangement, ammonia production rate of 9×10^{-9} mol cm^{-2} s^{-1} was observed at 750 °C. NEMCA effect (flux $\geq$I/2F) was observed which showed that H_2 required for ammonia synthesis can be supplied in the molecular form to the cathode as well as in form of H^+ pumped through the electrolyte. The pumped protons not only can directly participate in ammonia synthesis but also alter the work function of Pd catalyst to favour the chemical NH_3 formation reaction between gaseous hydrogen and nitrogen (conventional synthesis) at atmospheric pressure. As in a typical NEMCA phenomenon, the enhancement of catalytic activity here was attributed to the formation of the electrical double layer, reducing the activation potential for the catalysed reaction. In a similar study Skodra et al. employed an ammonia synthesis catalyst (Ru–MgO) to enhance the synthesis rate. They used a 1.5 mm thick ytterbium doped strontium cerate ($SrCe_{0.95}Yb_{0.05}O_{3-\delta}$ (SCY)) disc as the electrolyte [76]. Ru–MgO and Pd were respectively used as catalysts on the cathode and anode sides of the cell. Water on the anode side and nitrogen on the cathode side were used as reactants. The ammonia production rate of 4×10^{-13} mol cm^{-2} s^{-1} was observed at 650 °C and the low values of ammonia production rate were attributed to the unsuitability of the cathode catalyst and probably the poisoning effect of water on the anode catalyst.

Li et al. investigated ammonia synthesis by employing 0.8 mm thick samarium doped barium cerate ($BaCe_{0.9}Sm_{0.1}O_{3-\delta}$ (BCS)) and gadolinium + samarium doped barium cerate ($BaCe_{0.8}Gd_{0.1}Sm_{0.1}O_{3-\delta}$ (BCGS)) complex perovskites discs [77]. Ag–Pd was used as the catalyst on the anode as well as the cathode side of cells. Humidified hydrogen and dry nitrogen were used as reactants, and the ammonia production rates of 5.23×10^{-9} and 5.82×10^{-9} mol cm^{-2} s^{-1} respectively were observed for BCS and BCGS electrolytes at 620 °C. An operating voltage of 0.8 V was found to be optimal for the operation of the cell. Proton conduction was found to be better with wet H_2/dry N_2 as compared to wet H_2/dry air on the anode/cathode sides respectively of the membrane. In a separate study, Li et al. investigated ammonia synthesis with a 0.8 mm thick Gd doped barium cerate electrolyte [78]. The electrodes used were Ag–Pd similar to an earlier study [77]. The peak ammonia production rate achieved was 3.09×10^{-9} mol cm^{-2} s^{-1} at a significantly lower temperature of 480 °C, at an optimal cell operating voltage of 0.6 V. It was observed that an increase in temperature above 480 °C enhanced the proton conductivity of the electrolyte, but also lead to an increase in the decomposition rate of ammonia, resulting in a net reduction in the ammonia production rate. Liu et al. employed fluorite structured lanthanoids doped ceria based electrolytes for ammonia synthesis and studied the effect of dopant ion on the ammonia production rate [57]. They prepared a series of $Ce_{0.8}M_{0.2}O_{2-d}$ (M = La, Y, Gd, Sm) electrolyte cells with Ag–Pd as electrodes. The synthesis rates of 7.2×10^{-9}, 7.5×10^{-9}, 7.7×10^{-9} and 8.2×10^{-9} mol cm^{-2} s^{-1} were obtained for ceria doped with La, Y, Gd and Sm respectively with humidified H_2 (anode side) and dry N_2 (cathode side). An increasing synthesis rate in going from La to Sm in the series correlated well with the proton conductivity of each composition. These authors observed that the ammonia production rate increased linearly with increasing driving voltage up to 0.3 V and there was insignificant effect on synthesis rates above this voltage. Liu et al. attributed this behaviour to NEMCA effect which is significant at lower voltages while decreasing at higher voltages once catalyst adsorption limit is reached. Li et al. reported similar observations for electrolytic cells with complex perovskites [79]. They used $Ba_3(Ca_{1.18}Nb_{1.82})O_{9-\delta}$ (BCN18), $Ba_3CaZr_{0.5}Nb_{1.5}O_{9-\delta}$ (BCZN), and $Ba_3Ca_{0.9}Nd_{0.28}Nb_{1.82}O_{9-\delta}$ (BCNN) electrolyte pellets fabricated from powders prepared by wet chemical synthesis along with Ag–Pd electrodes. A maximum synthesis rate of 2.16×10^{-9} mol cm^{-2} s^{-1} was observed for a cell with BCNN electrolyte at 620 °C. The rate of ammonia formation increased rapidly with voltage till about 0.3 V and then more slowly, disappearing once the voltage reached 0.6 V. The limiting behaviour in production rates could be due to the NEMCA effect or the preferential evolution of molecular hydrogen at high currents or combination of both. These results clearly indicate the necessity of detailed studies on fundamental reaction mechanism and charge transfer steps in ammonia synthesis via the solid electrolytic routes. For fuel cell reactions, several detailed studies addressing these topics have been reported, however, such studies are not available for NH_3 synthesis.

Besides perovskites and fluorites, pyrochlores are also attractive candidates as low temperature proton conductors for ammonia synthesis as discussed earlier. Xie et al. reported ammonia synthesis with pyrochlore $La_{1.9}Ca_{0.1}Zr_2O_{6.95}$ proton conductor [80].The electrolyte was prepared with a sol–gel process and a fully dense electrolyte membrane was obtained on sintering at 1500 °C. With Ag–Pd electrodes, synthesis rates up to 1.76×10^{-9} mol cm^{-2} s^{-1} were reported at 520 °C with 80% of electrochemically supplied protons converted into NH_3. Wang et al. compared the synthesis rates between zirconate and cerate pyrochlores: Ca^{2+}-doped $La_2M_2O_7$ (M = Ce, Zr) [81]. With Ag–Pd electrodes the synthesis rates in these cells were 2×10^{-9} mol cm^{-2} s^{-1} and 1.3×10^{-9} mol cm^{-2} s^{-1} for $La_{1.95}Ca_{0.05}Zr_2O_7$ and $La_{1.95}Ca_{0.05}Ce_2O_7$ respectively at 520 °C. Higher ammonia production rates with $La_{1.95}Ca_{0.05}Zr_2O_7$ electrolyte, despite its lower total conductivity than $La_{1.95}Ca_{0.05}Ce_2O_7$, were attributed to mixed conduction in latter while the conduction was almost purely protonic in $La_{1.95}Ca_{0.05}Zr_2O_7$.

While various types of electrolytes have been tested for electrolytic NH_3 synthesis, the studies on electrode catalysts are limited. Conducting metals such as Ag–Pd or Pd appears to be preferred electrodes perhaps because of ease in preparation of electrochemical cells. Nevertheless an industrial Fe based catalyst has been studied by Ouzounidou et al. for ammonia synthesis [82]. These authors used 1.2 mm thick $SrZr_{0.95}Y_{0.05}O_{3-\delta}$ pellet as an electrolyte. The anode was prepared with silver paste while the cathode was prepared by first depositing a commercial iron paste on the pellet followed by a layer of commercial catalyst sintered at 800 °C. They observed electrochemical ammonia production rates of up to 0.65×10^{-11} mol cm^{-2} s^{-1}, in a double chamber reactor, at 450 °C and at 2 V cell voltage, with nitrogen and hydrogen gases supplied respectively to cathode and anode. The production rates were also compared with single chamber reactor cell with both H_2 and N_2 available at the cathode. More than 80% higher production rates were observed when protons

Table 2 – Ammonia production rates achieved with different electrolyte systems.

Electrolyte system	Operating temp.	NH_3 prod. rate (mol cm^{-2} s^{-1})	Ref.
$LiClO_4$ (0.2 M)) in tetrahydrofuran with ethanol as the H_2 source	50 °C	4.0×10^{-9}	[22]
Eutectic of LiCl, KCl and CsCl with Li_3N (0.5 mol%) as the source for nitride ions (N^{3-})	400 °C	3.3×10^{-9}	[26]
Li, Na, K – carbonate mixed with $LiAlO_2$ (50:50 wt. Ratio)	400 °C	2.32×10^{-10}	[32]
	450 °C	9.4×10^{-11}	
$Ce_{0.8}Sm_{0.2}O_{2-\delta}$ mixed with Li, Na, K – carbonate mixture (70:30 wt. ratio)	450 °C	5.39×10^{-9}	[34]
Yttrium doped ceria (YDC)–$Ca_3(PO_4)_2$–K_3PO_4 composite (80:20 wt% ratio)	650 °C	6.95×10^{-9}	[33]
Ytterbium doped strontium cerate ($SrCe_{0.95}Yb_{0.05}O_{3-\delta}$) (SCY)	570 °C	3.1×10^{-9} (Double chamber)	[74,75]
	750 °C	9×10^{-9} (Single chamber)	
Samarium doped barium cerate ($BaCe_{0.9}Sm_{0.1}O_{3-\delta}$ (BCS))	620 °C	5.23×10^{-9}	[77]
Gadolinium & samarium doped barium cerate ($BaCe_{0.8}Gd_{0.1}Sm_{0.1}O_{3-\delta}$ (BCGS))		5.82×10^{-9}	
Gadolinium doped barium cerate ($BaCe_{0.8}Gd_{0.2}O_{3-\delta}$ (BCG))	480 °C	3.09×10^{-9}	[78]
Ceria based electrolytes – $Ce_{0.8}M_{0.2}O_{2-\delta}$ (M = La, Y, Gd, Sm)	650 °C	7.2×10^{-9} to 8.2×10^{-9}	[57]
$Ba_3Ca_{0.9}Nd_{0.28}Nb_{1.82}O_9$ (BCNN) complex perovskite	620 °C	2.16×10^{-9}	[79]
$La_{1.9}Ca_{0.1}Zr_2O_{6.95}$ pyrochlore	520 °C	1.76×10^{-9}	[80]
Ca^{2+}-doped lanthanum cerate ($La_{1.95}Ca_{0.05}Ce_2O_7$)	520 °C	1.3×10^{-9}	[81]
Ca^{2+}-doped lanthanum zirconate ($La_{1.95}Ca_{0.05}Zr_2O_7$)		2×10^{-9}	
Yttrium doped strontium cerate ($SrZr_{0.95}Y_{0.05}O_{3-\delta}$)	450 °C	0.65×10^{-11}	[82]
Polymer membrane – Nafion	80 °C	1.13×10^{-8}	[97]
Sulfonated polysulfone (SPSF) membrane	80 °C	1.03×10^{-8}	[99]
Oxygen ion conducting 8 mol% Y_2O_3–ZrO_2 (O^{2-})	650 °C	3.8×10^{-13}	[76]

were electrochemically pumped through the electrolyte. Furthermore authors made an interesting observation and that is the poisoning of Fe catalyst by oxygen in double chamber reactor cells. In the absence of H_2 in the cathode chamber, minute oxygen content in the N_2 gas could oxidise the catalyst leading to reduction in its conversion efficiency. In the presence of hydrogen (which is the case in a single chamber cell), poisoning of catalyst is prevented by reaction between oxygen and hydrogen. If the oxygen content in the cathode chamber of a double chamber cell would have been the same as in a single chamber cell, further improvement in ammonia synthesis rates might have been observed. Earlier Yiokari et al. reported enhancement in the kinetics of ammonia synthesis reaction using industrial iron catalyst supported on a proton conductor in a single chamber reactor by the NEMCA effect [83]. They used 'BASF S6-10RED' catalyst mixed with iron paste applied on $CaIn_{0.1}Zr_{0.9}O_{3-\delta}$ pellet. Silver electrodes were used as counter and reference electrodes to complete the cell. Up to 13 fold enhancement in catalytic activity was reported under an electrical potential gradient which is a clear indication of the NEMCA effect, as also reported by other authors above. Under a voltage of −1 V, synthesis rate of up to about 4.9×10^{-9} mol cm^{-2} s^{-1} was achieved for a 24-pellet stack connected in parallel under a pressure of 50 bar assuming complete coverage of the electrolyte area by electrodes. The NEMCA effect was attributed to the promotion of protons on the catalysts surface in synergy with increased binding energy and sticking coefficient of N_2 on the catalyst surface because of negative potential on the surface of catalysts facilitating 'easier' adsorption of electron acceptor nitrogen [83]. Based on reported data, it is possible to achieve up to 50 °C reduction in operating temperature or a 30% reduction in operating pressure with such electrochemically promoted catalysts.

In summary, the literature review for electrochemical NH_3 synthesis utilising ceramic proton conducting membranes confirms that there is a significant potential of these systems for ammonia production with a number of electrolytes exhibiting reasonable proton conductivities (Table 2). However, the technology is still in the early stages of research and development and considerable efforts would be required to develop electrode catalysts for ammonia synthesis, electrolytes for sufficient proton conduction, understanding of fundamental reaction mechanism of NH_3 formation in these systems, long term stability and technology up-scaling with due regard to other system components.

7. Polymer membrane based systems

7.1. *Polymer electrolyte membrane materials*

There are various types of polymer ion exchange membranes available that can be used as an electrolyte in electrochemical ammonia synthesis cells. These are: perfluorosulfonic acid membranes such as Nafion from Dupont; Flemion from Asahi Glass; Aciplex from Asahi Chemical Industry; and Dow membranes from Dow Chemical. In addition there are hydrocarbon based membranes such as polyether ether ketone (PEEK) and polybenzimidazole (PBI). These membranes can be operated in the temperature range from room temperature to 120 °C.

Nafion membranes are the most popular proton conducting membranes being used in the chlor-alkali industry, and in the polymer electrolyte membrane (PEM) based fuel cells and electrolysis cells. Nafion membranes are produced by co-polymerisation of perfluoroalkyl sulfonyl fluoride with tetrafluoroethylene. These membranes are available in different equivalent weights which represent grams of dry membrane per mole of sulfonic acid. Most commonly used Nafion membranes (e.g. N112, N115, N117, N1135) have equivalent weight of 1100. The inverse of the equivalent weight represents the ion-exchange capacity of the membrane. The general chemical formula of Nafion and Flemion membranes is shown schematically in Fig. 11 [84]. The Nafion structure, generally agreed in the literature, is based on cluster-network model proposed by Hsu and Gierke [85] as shown in Fig. 12. It consists of approximately 4 nm diameter clusters of hydrophilic sulfonate ended perfluoroalkyl ether groups on hydrophobic tetrafluoroethylene backbone arranged as inverted micelles. These are joined to each other by approximately 1 nm diameter channels as shown in Fig. 12 and facilitate the proton transport between the clusters.

7.2. Proton conduction mechanism in polymer membranes

The proton conductivity of most polymer electrolyte membranes depends on the water content, equivalent weight, temperature and form (based on the type of conducting specie) of the membrane and it ranges from 0.01 to 0.1 S cm^{-1} [86]. There are two mechanisms proposed in the literature for proton transport in the polymer membranes – Grotthuss (hopping) mechanism and vehicle (diffusion) mechanism [84,86–88]. In Grotthuss mechanism protons are transferred from hydronium (H_3O^+) ions to water molecules, and the transfer continues from one neighbouring molecule to the next as schematically shown in Fig. 13(a). However, in the case of vehicle mechanism, it is the *en masse* diffusion of the hydronium ions that contributes to proton transport as shown in Fig. 13(b). A number of studies have been performed on proton transport in proton conducting polymer membranes [89,90] and based on above mechanisms, a parallel pore structural model has been proposed [86,88]. These pores or channels are formed by the nano separation of the hydrophilic proton exchange sites and hydrophobic fluorocarbon domains [91]. It has been suggested that when the water content in the membrane is low, there are less interaction amongst water molecules and strong electrostatic attraction between the protons and sulfonate ions. This leads to low rate of proton transfer in the membrane. This phenomenon is typically limited to the pore surface. However, with high water content, the properties of water in Nafion become quite similar to those in bulk water. Therefore, in the middle of the pores or when water content in the membrane is high, proton transfer is predominantly by Grotthuss mechanism, and the contribution by vehicle diffusion of hydronium ions to overall proton transfer is low. It has been found that in the H-form Nafion, vehicle mechanism dominates in the conduction of protons at higher temperature (85 °C), and Grotthuss mechanism prevails at low to medium temperatures [84,92].

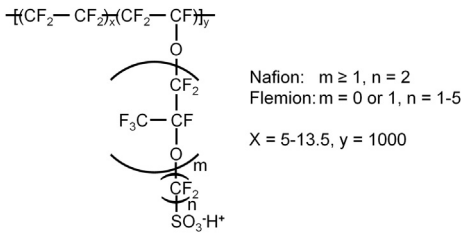

Fig. 11 – The general chemical formula of Nafion and Flemion membranes in H-state (Figure redrawn from Ref. [84]).

7.3. Ammonia synthesis with polymer membrane

There is limited information available in the open literature on the use of polymer membrane as an electrolyte in ammonia production cells. One of the main impediments for their use for ammonia synthesis is the degradation of acidic membranes such as Nafion in the presence of ammonia. It has been demonstrated recently by Hongsirikarn et al. that ammonium ion exchange with protons in Nafion membrane (fully exchanged ammonium form) results in reduction in the conductivity of the membrane by as much as 75–98% compared to proton-form membrane [87,93]. This observation has been also made by others on Nafion N117 and N105 membranes which showed that the conductivity of the fully protonated-form was four times than that of the ammonium-form [94,95]. Hongsirikarn et al. have suggested this to be due to the increase in the size of the cation (NH^{4+} being four times in radius than H^+) and the change in the ion transport mechanism [87,93]. This is in agreement with the observation made by others that the proton transport mainly occurs by faster hopping (Grotthuss) mechanism and bigger cations transport by slower diffusion (vehicle) mechanism [84]. It has been observed that the effect of ammonium ions in decreasing the conductivity of Nafion membrane can be reduced by increasing the level of humidification of the membrane. For example Hongsirikarn et al. tested Nafion N211 in H-form and ammonium-form at 80 °C [93]. It was found that the conductivity of ammonium-form membrane is lower than H-form by a factor of 55 and 3 respectively at 30%RH and 100%RH.

Despite some stability issues for polymer membranes in the presence of ammonia, there are enormous advantages of using these membranes due to their high proton conductivities at lower temperatures and a vast amount of information available for cell construction and assembly due to their usage in fuel cells. The low temperature operation would reduce the rate of decomposition of ammonia formed and avoid several other high temperature materials related issues. A schematic arrangement of the cell and its operation for ammonia synthesis employing proton conducting electrolyte membrane is shown in Fig. 3. This type of arrangement can be used with hydrogen as the reactant or water as the reactant for *in-situ* electrolysis to produce protons to participate in the ammonia synthesis reaction at the cathode.

Kordali et al. [96] were the first to demonstrate the electrochemical synthesis of ammonia at temperatures below 100 °C and at atmospheric pressures. Their cell consisted of ruthenium deposited on a carbon felt as the cathode catalyst in contact with Nafion membrane, platinum as the anode

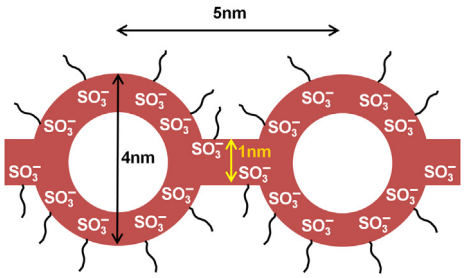

Fig. 12 – Cluster – network model for Nafion membranes (Figure redrawn from Ref. [85]).

catalyst, and 2 M KOH solution as the electrolyte. The anodic reaction was the oxygen evolution at the Pt electrode in contact with the KOH solution and the cathodic reaction was the reaction between the protons transported to the Nafion membrane and the nitrogen supplied at the Ru/carbon felt electrode in contact with the membrane. The observed maximum rate of ammonia synthesis was 2.12×10^{-11} mol cm^{-2} s^{-1} at 90 °C at a cathode voltage of −0.81 V (vs NHE), with an extremely low current efficiency (only 0.24%). The ammonia synthesis rate showed an Arrhenius relationship with temperature.

Xu et al. [97] investigated ammonia synthesis by using Nafion membrane102 as the electrolyte in a cell with $SmFe_{0.7}Cu_{0.3-x}Ni_xO_{3-\delta}$ (x = 0, 0.1, 0.2, 0.3) (SFCN) as the cathode catalyst and Ni-samarium doped ceria ($Ce_{0.8}Sm_{0.2}O_{2-\delta}$) (Ni-SDC) as the anode catalyst. In their investigation humidified hydrogen and dry nitrogen were used as the reactants on the anode and cathode side respectively. The set-up used for this investigation was similar to that shown schematically in Fig. 3. The ammonia synthesis measurements were made in the temperature range of 20–100 °C with cell voltage varying from 0.5 to 3 V. The best cathode catalyst that produced the highest ammonia production rate was $SmFe_{0.7}Cu_{0.1}Ni_{0.2}O_{3-\delta}$. The peak ammonia production rate achieved was 1.13×10^{-8} mol cm^{-2} s^{-1} at 80 °C, at an optimal cell operating voltage of 2 V, with a current efficiency of 90%. This is the highest ammonia generation rate so far reported by any

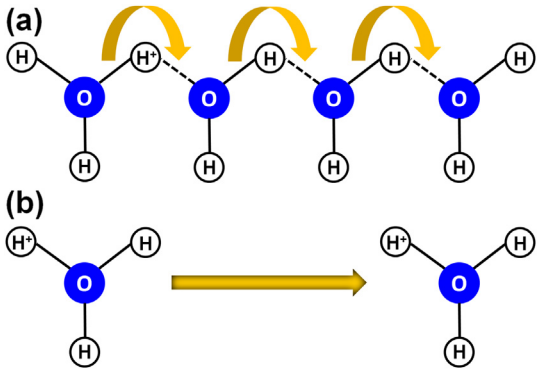

Fig. 13 – Schematic showing proton transport mechanism in perfluorosulfonated fully hydrated proton conducting membrane (a) Grotthuss (or hopping) mechanism; (b) Vehicle (or diffusion) mechanism (Figure redrawn from Ref. [84]).

investigator by employing a proton conducting polymer membrane. In another set of experiments, Xu et al. [98] investigated $Sm_{1.5}Sr_{0.5}MO_4$ (M represents Ni, Co or Fe) as the cathode catalyst compositions with other cell details same as mentioned above. The highest ammonia synthesis rate observed was 1.05×10^{-8} mol cm^{-2} s^{-1} with $Sm_{1.5}Sr_{0.5}NiO_4$ as the cathode catalyst, at 80 °C, and at cell operating voltage of 2.5 V. In a similar study, these authors [99] used an in-house synthesised sulfonated polysulfone (SPSF) electrolyte membrane with $Sm_{1.5}Sr_{0.5}NiO_4$ as the cathode catalyst. The peak ammonia synthesis rates measured were 1.03×10^{-8} mol cm^{-2} s^{-1} at 80 °C and at 2.5 V with SPSF membrane and these rates are comparable with those obtained with Nafion. Zhang et al. [100] by employing a similar electrolytic cell as mentioned above investigated ammonia synthesis rates with $SmBaCuMO_{5+\delta}$ (M represents Ni, Co or Fe) as the cathode catalyst compositions. $SmBaCuNiO_{5+\delta}$ catalyst was found to produce the highest ammonia production rates. The peak rate achieved with this catalyst was 0.87×10^{-8} mol cm^{-2} s^{-1} at 80 °C, at an optimal cell operating voltage of 2.5 V.

Hasnat et al. [101] synthesised ammonia by reducing nitrate/nitrite over Pd based bi-metallic catalysts deposited on a Nafion N117 proton conducting polymer membrane. In this cell, the bimetallic catalyst deposited on one side of the membrane acted as the cathode and the Pt deposited on the other side acted as the anode. Water and nitrate/nitrite solution were provided as reactants respectively in the anode and cathode chambers (separated by the polymer electrolyte membrane) of the cell. Water dissociates on the anode side to produce protons, which on migration through the Nafion membrane react at the cathode with nitrate/nitrite ions to form ammonium ions. In order to compare the reduction rates in a conventional reactor, catalysts deposited on the Nafion membrane (which was used here only as a catalyst support) acted as the anode and the cathode without the presence of Nafion electrolyte membrane in the middle. Instead the nitrate/nitrite solution in water was provided between the two electrodes for the conventional ammonia synthesis. For both cases, the solutions were analysed for NO_3^-, NO_2^- and NH_4^+ concentrations during 180 min of electrolysis (at 100 mA). For most bimetallic catalysts in the electrolytic reactor with Nafion as the electrolyte membrane, ammonium concentration generally increased and nitrate concentration decreased, whereas nitrite concentration initially increased and then decreased with time. For Rh–Pd bimetallic electrode, the KNO_2 reduction rate constant was significantly higher (by an order of magnitude) in the case of electrolytic reactor in comparison to the conventional reactor. Furthermore, the electrolyte reactor produced higher ammonium concentration compared to the conventional reactor. Apart from this report, there is no other information available on the ammonia production rates or the viability of the process.

8. O^{2-} conducting membrane materials and ammonia synthesis systems

A large number of O^{2-} conducting ceramic electrolytes are available and have been used in oxygen sensors, solid oxide

fuel cells and for high temperature steam electrolysis. These include fully and partially stabilised ZrO_2 with different dopant types and levels, doped CeO_2, doped $LaGaO_3$ at A- and B-sites, and doped Bi_2O_3 [102]. The O^{2-} conductivity as a function of temperature for main electrolyte materials is shown in Fig. 8. The O^{2-} conductivity regime varies significantly with the type of material used. Although some of these materials retain O^{2-} conductivity over a wide range of temperatures, oxygen partial pressures and gas compositions, others develop either electronic or even proton conductivity in the presence of water and similar to those reported for doped $BaSrO_3$ and $SrCeO_3$ by Iwahara [39,41]. The use of such materials, despite being O^{2-} conductors in air, has been explored as proton conductors for ammonia production as discussed in Section 6.1. In principle, electrolyte materials which remain as pure O^{2-} conductors even in the presence of hydrogen and water vapours can be used for ammonia production as shown in Fig. 14 [20]. However, there is very little information available on such systems apart from a publication by Skodra and Stoukides [76] where they employed 8 mol% Y_2O_3–ZrO_2 electrolyte, a silver anode and commercial Ru–MgO catalyst on top of a thin Pd layer as the cathode. The Pd layer was used as it is known to be a good catalyst for water dissociation and also to enhance cathode conductivity as Ru–MgO catalyst has poor conductivity. N_2 and H_2O (steam) were fed to the cathode and He to the anode or oxygen evolution side with reactions under electric load as shown in Fig. 14. The ammonia production rates at a constant voltage of 2 V (~17 mA) was determined to be $\sim 3.8 \times 10^{-13}$ mol cm^{-2} s^{-1} at 650 °C. The very low ammonia production rates were attributed to the nature of the catalyst used on the cathode side including its low electrical conductivity. However, the novelty of the concept is that steam was used as the source of hydrogen rather than hydrogen from reforming of natural gas followed by purification. With the use of better conducting electrolytes such as Sc_2O_3–ZrO_2, which have significantly higher conductivity than Y_2O_3–ZrO_2, and the development of cathode catalyst, there is a potential to improve ammonia production rates.

9. Current technical issues and status of electrochemical methods

The merit of any electrochemical route for ammonia synthesis can be judged from two parameters initially. These are the ammonia production rate (the total amount of ammonia produced per unit cell area per unit time usually measured in mol cm^{-2} s^{-1}) and conversion rate related to current efficiency of the process. The current efficiency is defined by how much of the current that flows through the cell actually goes towards ammonia production.

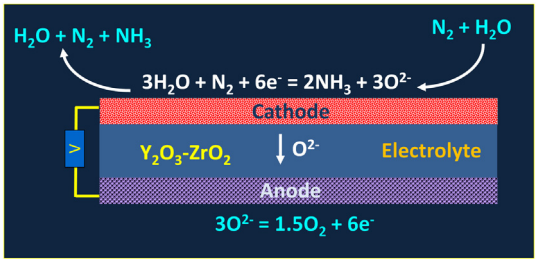

Fig. 14 – A schematic of the operating principle of electrochemical route for ammonia synthesis based on O^{2-} conducting solid electrolyte which does not develop proton conductivity in the presence of H_2/H_2O.

Most of the requirements on the electrode, electrolyte and interconnect (for multiple cell construction) materials in terms of their conductivity, and thermal and mechanical properties are similar to those for fuel cells. However, N_2 is a difficult molecule to break requiring cleavage of three bonds. The competing H_2 evolution reaction is often favoured compared to NH_3 formation due to the easier recombination of the adsorbed H atoms as compared to the reaction between adsorbed H atoms and N_2 molecules due to the stronger N≡N triple bond. Therefore, the requirements for the catalyst material on the ammonia synthesis side are quite stringent.

Table 2 shows the ammonia production rates achieved by electrochemical methods employed by different investigators and for different electrolyte systems. The ammonia production rates achieved so far are in the range of 10^{-13}–10^{-8} mol cm^{-2} s^{-1}. These ammonia synthesis rates are too low and are due to H^+ flux or transport number t_{H+} being too low through the electrolytes, or the slow reaction kinetics at the electrode/electrolyte interface on the ammonia production side. Although increasing the temperature of operation can enhance the synthesis rates, the rate of thermal decomposition of ammonia also increases. It has been observed by many investigators that the transport number t_{H+} in ceramic proton conductors is a function of the temperature of operation, type of gases on both sides of the cell and the current density. Furthermore, the conversion efficiencies (H^+ to NH_3) are generally low when hydrogen flux through the electrolyte is high. Alternatively high conversion efficiencies in excess 50% have been reported, however, ammonia production rates are very low due to very low reactive specie flux (current flow) through the electrolyte. Thus low ammonia production rates would require much larger active area cells and moreover separation of ammonia and recycling of unreacted hydrogen would further add to the plant size and cost.

The highest ammonia production rate reported so far is 1.13×10^{-8} mol cm^{-2} s^{-1} by employing a proton conducting polymer electrolyte membrane (Nafion). The catalyst used on the cathode side of the cell was $SmFe_{0.7}Cu_{0.3-x}Ni_xO_3$. However, there are concerns of using an acid based electrolyte with ammonia, the performance of which is known to degrade with time. These high flux rates, although quite encouraging, are likely to have been achieved over a very short period of operation.

If it would be possible to achieve current densities somewhat similar to those achieved in fuel cells or electrolysis cells (0.25–0.5 A cm^{-2}) with around 50% current efficiency or hydrogen conversion rates, then ammonia production rates in the range $4.3–8.7 \times 10^{-7}$ mol cm^{-2} s^{-1} can be achieved. These would be quite reasonable for commercial systems, however, substantial improvements to cell materials (catalyst and electrolyte) would be required to achieve such rates.

Other factors that need to be considered are cell material and component fabrications costs, operating conditions and

life time. If any precious metal catalysts such as those based on Pd or Ru are to be used, then the quantity of catalyst required per unit cell or catalysts loading should be kept to a minimum. Typically, electrochemical routes, investigated so far require operation at much lower pressures than those used in the Haber–Bosch process with operating temperatures from near room temperature for liquid and polymer electrolyte systems to between 400 and 800 °C for other solid electrolytic routes. The low temperature operation has the potential to reduce material and operating costs and increase life time of the electrochemical reactor provided high ammonia production rates and high current efficiency can be achieved. However, one significant advantage of ammonia production by high temperature electrolytic routes is that such systems can be integrated with solar (renewable energy), thermal or nuclear power plants to provide the waste heat for high temperature operation thus reducing the overall energy input especially if water is used as the hydrogen source. In addition to natural gas being a source of hydrogen, it can also be supplied by water electrolysis [21,103–105]. Several routes for hydrogen generation via electrolytic routes are available and discussed in recent review articles [104,106]. The process can be carried out under ambient conditions or at higher temperatures depending on the type of the electrolyte material used. Water can also act as a source of protons within the electrolytic cell through its reaction in the electrochemical process as shown in Fig. 3. This has the potential to reduce plant cost by using only a single reactor to perform hydrogen generation and conversion tasks.

So far there is very little economic assessment of electrolytic routes for ammonia production. Furthermore there is not much information available on the degradation rates and long term stability of most materials and electrochemical cells in ammonia containing environments. This is not surprising in view of the early stage of development of the science and technology in this area.

10. Conclusion

The paper covers a review of literature on various electrochemical methods for ammonia synthesis and cell materials. The ammonia synthesis rates are generally low (in the range of 10^{-13}–10^{-8} mol cm^{-2} s^{-1}). The maximum ammonia production rate observed was around 10^{-8} mol cm^{-2} s^{-1} with a polymer electrolyte membrane. While these are encouraging, the long term stability of the acidic electrolyte membranes is a concern. Furthermore, for most data reported on electrochemical processes for ammonia production, high current efficiency is achieved at the expense of low ammonia production rates. The ceramic proton conducting materials with suitable cathode catalysts (ammonia production side) show promise worthy of further investigations in the area. It is concluded that while there is a substantial scope for the development of electrochemical processes for ammonia synthesis, and the low pressure operation is an advantage, the technology is at an early stage of research and development requiring significant advances in catalysts on ammonia production side, development of other materials of construction and optimisation of operating conditions. Most of the literature work is reported on single cells. Although, stacking configurations used for fuel cells and water or steam electrolysers are of direct relevance, the research and development on electrochemical ammonia production routes has not advanced to multi-cell or module testing. Early economic assessment of various electrochemical routes is desirable to make valid comparison with the Haber–Bosch process.

Acknowledgements

Authors would like to thank Dr Christopher Munnings for reviewing this manuscript.

REFERENCES

[1] Appl M. Ammonia principles and industrial practice. New York: Wiley-VCH; 2007.
[2] Medard L. Air Liquide Gas Encyclopaedia. Amsterdam: Elsevier; 1976. 3rd ed.: 2002. ISBN: 0444 41492 4, English translation by Marshall N, http://encyclopedia.airliquide.com/Encyclopedia.asp?GasID=2 [cited 24 April 2013].
[3] Avery WH. A role for ammonia in hydrogen economy. Int J Hydrogen Energy 1988;13:761–73.
[4] Haber F. The synthesis of ammonia from its elements nobel lecture. Available at: www.nobelprize.org/nobel_prizes/chemistry/laureates/1918/haber-lecture.pdf; 1920 [cited 24 April 2013].
[5] Topham SA. The history of the catalytic synthesis of ammonia. In: Anderson JR, Boudart M, editors. Catalysis science and technology. Berlin-Heidelberg: Springer-Verlag; 1985. p. 1–50.
[6] Modak JM. Haber process for ammonia synthesis. Resonance 2011;16:1159–67.
[7] Anantharaman B, Hazarika S, Ahmad T, Nagvekar M, Ariyapadi S, Gualy R. Coal gasification technology for ammonia plants. In: Asia nitrogen & syngas 2012 conference. Kuala Lumpur, Malaysia. Available at: http://www.kbr.com/Newsroom/Publications/Whitepapers/Coal-Gasification-Technology-for-Ammonia-Plants.pdf; Oct 2012 [cited 24 April 2013].
[8] Market study: ammonia (UC-3705). Cerasena Market Intelligence Consulting; October 2012. p. 530. Available at: http://www.ceresana.com/en/market-studies/chemicals/ammonia/ceresana-market-study-ammonia.html [cited 24 April 2013].
[9] Lipman T, Shah N. Ammonia as an alternative energy storage medium for hydrogen fuel cells: scientific and technical review for near-term stationary power demonstration projects. Final report. UC Berkeley: UC Berkeley Transportation Sustainability Research Centre, Institute of Transportation Studies (UCB); 11-01-2007. Available at:, http://www.escholarship.org/uc/item/7z69v4wp [cited 24 April 2013].
[10] Schiller M. Industrial uses of ammonia. Available at: http://www.easychem.com.au/monitoring-and-management/maximising-production/industrial-uses-of-ammonia [cited 24 April 2013].
[11] Holladay JD, Hu J, King DL, Wang Y. An overview of hydrogen production technologies. Catal Today 2009;139:244–60.
[12] Lan R, Irvine JTS, Tao S. Ammonia and related chemicals as potential indirect hydrogen storage materials. Int J Hydrogen Energy 2012;37:1482–94.

[13] Christensen CH, Johannessen T, Sørensen RZ, Nørskov JK. Towards an ammonia-mediated hydrogen economy. Catal Today 2006;111:140–4.

[14] Thomas G, Parks G. Potential roles of ammonia in a hydrogen economy. A study related to the use of ammonia for on-board vehicular hydrogen storage. U.S. Department of Energy; 2006. http://www.hydrogen.energy.gov/pdfs/nh3_paper.pdf [cited 24 April 2013].

[15] Practical, carbon-free fuel. In: 9th annual NH_3 fuel association conference, San Antonio, Texas, USA. http://nh3fuelassociation.org/nh3-fuel-association/; 30 September–3 October 2012 [cited 24 April 2013].

[16] Hejze T, Besenhard JO, Kordesch K, Cifrain M, Aronsson RR. Current status of combined systems using alkaline fuel cells and ammonia as a hydrogen carrier. J Power Sources 2008;176:490–3.

[17] Fuerte A, Valenzuela RX, Escudero MJ, Daza L. Ammonia as efficient fuel for SOFC. J Power Sources 2009;192:170–4.

[18] Zhang L, Yang W. Direct ammonia solid oxide fuel cell based on thin proton conducting electrolyte. J Power Sources 2008;179:92–5.

[19] Pelletier L, McFarlan A, Maffei N. Ammonia fuel cell using doped barium cerate proton conducting solid electrolyte. J Power Sources 2005;145:262–5.

[20] Amar IA, Lan R, Petit CTG, Tao S. Solid-state electrochemical synthesis of ammonia: a Review. J Solid State Electrochem 2011;15:1845–60.

[21] Clarke RE, Giddey S, Ciacchi FT, Badwal SPS, Paul B, Andrews J. Direct coupling of an electrolyser to a solar PV system for generating hydrogen. Int J Hydrogen Energy 2009;34:2531–42.

[22] Tsuneto A, Kudo A, Sakata T. Lithium-mediated electrochemical reduction of high pressure N_2 to NH_3. J Electroanal Chem 1994;367:183–8.

[23] Pappenfus TM, Lee K, Thoma LM, Dukart CR. Wind to ammonia: electrochemical processes in room temperature ionic liquids. ECS Trans 2009;16:89–93.

[24] Köleli F, Kayan DB. Low overpotential reduction of dinitrogen to ammonia in aqueous media. J Electroanal Chem 2010;638:119–22.

[25] Köleli F, Röpke D, Aydin R, Röpke T. Investigation of N_2-fixation on polyaniline electrodes in methanol by electrochemical impedance spectroscopy. J Appl Electrochem 2011;41:405–13.

[26] Murakami T, Nishikiori T, Nohira T, Ito Y. Electrolytic synthesis of ammonia in molten salts under atmospheric pressure. J Am Chem Soc 2003;125:334–5.

[27] Murakami T, Nohira T, Ogata YH, Ito Y. Electrolytic ammonia synthesis in molten salts under atmospheric pressure using methane as a hydrogen source. Electrochem Solid State Lett 2005;8:D12–4.

[28] Murakami T, Nohira T, Goto T, Ogatab YH, Ito Y. Electrolytic ammonia synthesis from water and nitrogen gas in molten salt under atmospheric pressure. Electrochim Acta 2005;50:5423–6.

[29] Murakami T, Nohira T, Araki Y, Goto T, Hagiwara R, Ogata YH. Electrolytic synthesis of ammonia from water and nitrogen under atmospheric pressure using a boron-doped diamond electrode as a non-consumable anode. Electrochem Solid State Lett 2007;10:E4–6.

[30] Murphy OJ, Denvir AJ, Teodorescu SG, Uselton KB. Electrochemical synthesis of ammonia. US Patent 7314544 B2; 2008.

[31] Di J, Chen M, Wang C, Zheng J, Fan L, Zhu B. Samarium doped ceria–$(Li/Na)_2CO_3$ composite electrolyte and its electrochemical properties in low temperature solid oxide fuel cell. J Power Sources 2010;195:4695–9.

[32] Amar IA, Lan R, Petit CTG, Arrighi V, Tao S. Electrochemical synthesis of ammonia based on a carbonate-oxide composite electrolyte. Solid State Ion 2011;182:133–8.

[33] Wang BH, Wang JD, Liu RQ, Xie YH, Li ZJ. Synthesis of ammonia from natural gas at atmospheric pressure with doped ceria-$Ca_3(PO_4)_2$-K_3PO_4 composite electrolyte and its proton conductivity at intermediate temperature. J Solid State Electrochem 2006;11:27–31.

[34] Amar IA, Petit CTG, Zhang L, Lan R, Skabara PJ, Tao S. Electrochemical synthesis of ammonia based on doped-ceria-carbonate composite electrolyte and perovskite cathode. Solid State Ion 2011;201:94–100.

[35] Kreuer KD. Proton conducting oxides. Annu Rev Mater Res 2003;33:333–9.

[36] Phair JW, Badwal SPS. Review of proton conductors for hydrogen separation. Ion 2006;12:103–15.

[37] Stotz S, Wagner C. Die Losiichkeit von Wasserdampf und Waeserstoff in festen Oxiden Bunsenges. B Physik Chem 1966;70:781–8.

[38] Shores DA, Rapp RA. Hydrogen ion (proton) conduction in thoria-base solid electrolytes. J Electrochem Soc 1972;119:301–5.

[39] Iwahara H, Esaka T, Uchida H, Maeda N. Proton conduction in sintered oxides and its application to steam electrolysis. Solid State Ion 1981;3–4:359–63.

[40] Wu J. Defect chemistry and proton conductivity in Ba-based perovskites. Ph.D. Thesis. California Institute of Technology; 2005.

[41] Katahira K, Kohchi Y, Shimura T, Iwahara H. Protonic conduction in Zr-substituted $BaCeO_3$. Solid State Ion 2000;138:91–8.

[42] Reijers R, Haije W. Literature review on high temperature proton conducting materials. Energy Research Centre of Netherlands; 2008. Number: ECN-E–08-091. Available at: www.ecn.nl/publicaties/PdfFetch.aspx?nr=ECN-E–08-091 [cited 24 April 2013].

[43] Iwahara H. Technological challenges in the application of proton conducting ceramics. Solid State Ion 1995;77:289–98.

[44] Norby T. Proton conductivity in perovskite oxides. In: Ishihara T, editor. Perovskite oxide for solid oxide fuel cells, fuel cells and hydrogen energy. Springer Science & Business Media; 2009. p. 217–24.

[45] Nowick A, Du Y. High-temperature protonic conductors with perovskite-related structures. Solid State Ion 1995;77:137–46.

[46] Bhide SV, Virkar AV. Stability of $AB'_{1/2}B''_{1/2}O_3$-type mixed perovskite proton conductors. J Electrochem Soc 1999;146:4386–92.

[47] Liang KC, Nowick AS. Fast high-temperature proton transport in nonstoichiometric mixed perovskites. Solid State Ion 1994;69:117–20.

[48] Nowick AS, Du Y, Liang KC. Some factors that determine proton conductivity in nonstoichiometric complex perovskites. Solid State Ion 1999;125:303–11.

[49] Babilo P, Haile SM. Enhanced sintering of yttrium doped barium zirconate by addition of ZnO. J Am Ceram Soc 2005;88:2362–8.

[50] Bia L, Zhanga S, Zhangb L, Taoa Z, Wangb H, Liu W. Indium as an ideal functional dopant for a proton-conducting solid oxide fuel cell. Int J Hydrogen Energy 2009;34:2421–5.

[51] Zhaoa F, Liua Q, Wanga S, Brinkmanb K, Chen F. Synthesis and characterization of $BaIn_{0.3}L_xY_xCe_{0.7}O_3Ld$ (x [0, 0.1, 0.2, 0.3]) proton conductors. Int J Hydrogen Energy 2010;35:4258–63.

[52] Park YS, Lee JH, Lee HW, Kim BK. Low temperature sintering of $BaZrO_3$-based proton conductors for intermediate temperature solid oxide fuel cells. Solid State Ion 2008;181:163–7.

[53] Tao S, Irvine JTS, Stable A. Easily sintered proton-conducting oxide electrolyte for moderate-temperature fuel cells and electrolysers. Adv Mater 2006;18:1581–4.

[54] Suna W, Zhua Z, Shia Z, Liu W. Chemically stable and easily sintered high-temperature proton conductor $BaZr_{0.8}In_{0.2}O_{3-\delta}$ for solid oxide fuel cells. J Power Sources 2013;229:95–101.

[55] Magraso A, Kjølseth C, Haugsrud R, Norby T. Influence of Pr substitution on defects, transport, and grain boundary properties of acceptor-doped $BaZrO_3$. Int J Hydrogen Energy 2012;37:7962–9.

[56] Chen C, Ma G. Preparation, proton conduction, and application in ammonia synthesis at atmospheric pressure of $La_{0.9}Ba_{0.1}Ga_{1-x}Mg_xO_{3-\alpha}$. J Mater Sci 2008;43:5109–14.

[57] Liu R, Xie Y, Wang J, Li ZJ, Wang B. Synthesis of ammonia at atmospheric pressure with $Ce_{0.8}M_{0.2}O_{2-\delta}$ (M = La, Y, Gd, Sm) and their proton conduction at intermediate temperature. Solid State Ion 2006;177:73–6.

[58] Shimura T, Fujimoto S, Iwahara H. Proton conduction in non-perovskite-type oxides at elevated temperatures. Solid State Ion 2001;143:117–23.

[59] Omata T, Matsuo SO. Electrical properties of proton-conducting Ca^{2+} doped $La_2Zr_2O_7$ with a pyrochlore-type structure. J Electrochem Soc 2001;148:E252–61.

[60] Fontaine M, Norby T, Larring Y, Grande T, Bredesen R. Oxygen and hydrogen separation membranes based on dense ceramic conductors. In: Mallada R, Menéndez M, editors. Membrane science and technology. Elsevier; 2008. p. 401–58.

[61] Malavasi L, Fisherb CAJ, Islam M. Oxide-ion and proton conducting electrolyte materials for clean energy applications: structural and mechanistic features. Chem Soc Rev 2010;39:4370–87.

[62] Nyman J. Proton conductivity of lanthanum and barium zirconate. Ph.D. Thesis. Sweden: Chalmers University of Technology; 2012.

[63] Carlson M. Perspectives of neutron scattering on proton conducting oxides. Dalton Trans 2013;42:317–29.

[64] Munch W, Kreuer KD, Adams ST, Seifert S, Maier J. The relation between structure and the formation and mobility of protonic charge carries in perovskite-type oxides: a case study of Y doped $BaCeO_3$ and $SrCeO_3$. Phase Trans;68:567–86.

[65] Kreuer KD. Aspects of the formation and mobility of protonic charge carriers and the stability of perovskite-type oxides. Solid State Ion 1999;125:285–302.

[66] Larring Y, Norby T. Protons in rare earth oxides. Solid State Ion 1995;77:147–215.

[67] De Souzaa RA, Munirb ZA, Kimb S, Martina M. Defect chemistry of grain boundaries in proton-conducting solid oxides. Solid State Ion 2011;196:1–8.

[68] Kim S, Paredes H, Wang S, Chen C, De Souza RA, Martin M, et al. On the conduction pathway for protons in nanocrystalline yttria-stabilized zirconia. Phys Chem Chem Phys 2009;11:3035–8.

[69] Haile SM, Staneff G, Ryu KH. Non-stoichiometry, grain boundary transport and chemical stability of proton conducting perovskites. J Mater Sci 2001;36:1149–60.

[70] Paredes HJ, Chen C, Wang S, Souza R, Martin M, Kim S. Grain boundaries in dense nanocrystalline ceria ceramics: exclusive pathways for proton conduction at room temperature. J Mater Chem 2010;20:10110–2.

[71] Kulkarni A, Dong J, Bourandas A, Fuierer PA, Xiao H. A nanocrystalline $(Zr_{0.84}Y_{0.16})O_{1.92}$-$(Ce_{0.85}Sm_{0.15})O_{1.925}$ heterophase thin film and its electrical conductivity. J Mater Res 2006;21:500–4.

[72] Azad S, Marina OA, Wang CM, Saraf L, Shutthanandan V, McCready DE, et al. Nanoscale effects on ion conductance of layer-by-layer structures of gadolinia-doped ceria and zirconia. Appl Phys Lett 2005;86:131906-1–131906-2.

[73] Panagos E, Voudouris I, Stoukides M. Modelling of equilibrium limited hydrogenation reactions carried out in H^+ conducting solid oxide membrane reactors. Che Eng Sci 1996;51:3175–80.

[74] Marnellos G, Zisekas S, Stoukides M. Synthesis of ammonia at atmospheric pressure with the use of solid state proton conductors. J Catal 2000;193:80–7.

[75] Marnellos G, Stoukides M. Ammonia synthesis at atmospheric pressure. Science 1998;282:98–100.

[76] Skodra A, Stoukides M. Electrocatalytic synthesis of ammonia from steam and nitrogen at atmospheric pressure. Solid State Ion 2009;180:1332–6.

[77] Li Z, Liu R, Wang J, Xu Z, Xie Y, Wang B. Preparation of double-doped $BaCeO_3$ and its application in the synthesis of ammonia at atmospheric pressure. Sci Tech Adv Mater 2007;8:566–70.

[78] Li Z, Liu R, Wang J, Xie Y. Preparation of $BaCe_{0.8}Gd_{0.2}O_{3-\delta}$ by the citrate method and its application in the synthesis of ammonia at atmospheric pressure. J Solid State Electrochem 2005;9:201–4.

[79] Li Z, Liu R, Xie Y, Feng S, Wang J. A novel method for preparation of doped $Ba_3(Ca_{1.18}Nb_{1.82})O_{9-\delta}$: application to ammonia synthesis at atmospheric pressure. Solid State Ion 2005;176:1063–6.

[80] Xie Y, Wang J, Liu R, Su X, Sun Z, Li Z. Preparation of $La_{1.9}Ca_{0.1}Zr_2O_{6.95}$ with pyrochlore structure and its application in synthesis of ammonia at atmospheric pressure. Solid State Ion 2004;168:117–21.

[81] Wang J, Xie Y, Zhang Z, Liu R, Li Z. Protonic conduction in Ca^{2+}-doped $La_2M_2O_7$ (M = Ce, Zr) with its application to ammonia synthesis electrochemically. Mater Res Bull 2005;40:1294–302.

[82] Ouzounidou M, Skodra A, Kokkofitis C, Stoukides M. Catalytic and electrocatalytic synthesis of NH_3 in a H^+ conducting cell by using an industrial Fe catalyst. Solid State Ion 2007;178:153–9.

[83] Yiokari CG, Pitselis GE, Polydoros DG, Katsaounis AD, Vayenas CG. High-pressure electrochemical promotion of ammonia synthesis over an industrial iron catalyst. J Phys Chem 2000;104:10600–2.

[84] Saito M, Hayamizu K, Okada T. Temperature dependence of ion and water transport in perfluorinated ionomer membranes for fuel cells. J Phys Chem 2005;B 109:3112–9.

[85] Hsu WY, Gierke TD. Ion transport and clustering in Nafion perfluorinated membranes. J Memb Sci 1983;13:307–26.

[86] Choi P, Jalani NH, Datta R. Thermodynamics and proton transport in Nafion – II. Proton diffusion mechanisms and conductivity. J Electrochem Soc 2005;152:E123–30.

[87] Hongsirikarn K. Effect of impurities on performance of proton exchange membrane fuel cell components. Ph.D. Thesis. USA: The Graduate School of Clemson University; 2010. Available at:, http://etd.lib.clemson.edu/documents/1306858565/Hongsirikarn_clemson_0050D_11038.pdf [cited 24 April 2013].

[88] Sahu AK, Pitchumani S, Sridhar P, Shukla AK. Nafion and modified-Nafion membranes for polymer electrolyte fuel cells: an overview. Bull Mater Sci 2009;32:285–94.

[89] Wirguin CH. Recent advances in perfluorinated ionomer membranes: structure, properties and applications. J Memb Sci 1996;120:1–33.

[90] Mauritz KA, Moore RB. State of understanding of Nafion. Chem Rev 2004;104:4535–85.

[91] Kreuer KD. On the development of proton conducting polymer membranes for hydrogen and methanol fuel cells. J Memb Sci 2001;185:29–39.

[92] Lott KF, Ghosh BD, Ritchie JE. Measurement of anion diffusion and transference numbers in an anhydrous proton conducting electrolyte. Electrochem Solid State Lett 2005;8:A513–5.
[93] Hongsirikarn K, Goodwin Jr JG, Greenway S, Creager S. Influence of ammonia on the conductivity of Nafion membranes. J Power Sources 2010;195:30–8.
[94] Uribe FA, Gottesfeld S, Zawodzinski Jr TA. Effect of ammonia as potential fuel impurity on proton exchange membrane fuel cell performance. J Electrochem Soc 2002;149:A293–6.
[95] Halseid R, Vie PJS, Tunold R. Influence of ammonium on conductivity and water content of Nafion 117 membranes. J Electrochem Soc 2004;151:A381–8.
[96] Kordali V, Kyriacou G, Lambrou C. Electrochemical synthesis of ammonia at atmospheric pressure and low temperature in a solid polymer electrolyte cell. Chem Commun 2000;31:1673–4.
[97] Xu G, Liu R, Wang J. Electrochemical synthesis of ammonia using a cell with a Nafion membrane and $SmFe_{0.7}Cu_{0.3-x}Ni_xO_3$ ($x = 0$–0.3) cathode at atmospheric pressure and lower temperature. Sci China Ser B Chem 2009;52:1171–5.
[98] Xu G, Liu R. $Sm_{1.5}Sr_{0.5}MO_4$ (M = Ni, Co, Fe) cathode catalysts for ammonia synthesis at atmospheric pressure and lower temperature. Chinese J Chem 2009;27:677–80.
[99] Liu R, Xu G. Comparison of electrochemical synthesis of ammonia by using sulfonated polysulfone and Nafion membrane with $Sm_{1.5}Sr_{0.5}NiO_4$. Chinese J Chem 2010;28:139–42.
[100] Zhang Z, Zhong Z, Liu R. Cathode catalysis performance of $SmBaCuMO_{5+\delta}$ (M = Fe, Co, Ni) in ammonia synthesis. J Rare Earths 2010;28:556–9.
[101] Hasnat MA, Karim MR, Machida M. Electrocatalytic ammonia synthesis: role of cathode materials and reactor configuration. Catal Commun 2009;10:1975–9.
[102] Badwal SPS, Ciacchi FT. Oxygen-ion conducting electrolyte materials for solid oxide fuel cells. Ionics 2000;6:1–21.
[103] Grundt T, Christiansen K. Hydrogen by water electrolysis as basis for small scale ammonia production. A comparison with hydrocarbon based technologies. Int J Hydrogen Energy 1982;7:247–57.
[104] Badwal SPS, Giddey S, Munnings C. Hydrogen production via solid electrolytic routes. WIREs Energy Environ 2013;2:473–87. http://dx.doi.org/10.1002/wene.50.
[105] Lan R, Irvine JTS, Tao S. Synthesis of ammonia directly from air and water at ambient temperature and pressure. Sci Rep;3:1145. http://dx.doi.org/10.1038/srep01145(2013).
[106] Smolinka T. Fuels – water electrolysis. In: Encyclopaedia of electrochemical power sources. Garche J, editor-in-chief. Elsevier B.V. Amsterdam; 2009; 3: 394–413.